AD NUMBER
AD394650
CLASSIFICATION CHANGES
TO: unclassified
FROM: confidential
LIMITATION CHANGES
TO: Approved for public release, distribution unlimited
FROM: Distribution authorized to DoD only; Specific Authority; 27 NOV 1968. Other requests shall be referred to Naval Air Systems Command, Washington, DC 20360.
AUTHORITY
Nrl ltr, 4 Aug 1982; NRL ltr, 4 Aug 1982

AD NUMBER

AD394650

CLASSIFICATION CHANGES

TO

confidential

FROM

secret

AUTHORITY

30 Nov 1971, DoDD 5200.10

AD- 394650

SECURITY REMARKING REQUIREMENTS

DOD 5200.1-R, DEC 78

REVIEW ON 27 NOV 88

SECURITY MARKING

The classified or limit d status of this report applies to each page, unless otherwise marked.
Separate page printouts MUST be marked accordingly.

NRL Report 6804
Copy No.

Ocean Surveillance Statistical Considerations

(Unclassified Title)

A. V. [illegible]

Radar Analysis Staff
Radar Division

November 27, 1968

NAVAL RESEARCH LABORATORY
Washington, D.C.

SECRET

CONTENTS

ABSTRACT
[Secret]

Several statistical topics were studied concerning detection of targets on the ocean's surface from a satellite-based radar. First, a desired signal-to-noise ratio was obtained by considering the tradeoff between false alarms and detected targets. For a 0.99 detection probability and a 10^{-10} false alarm probability the S/N ratio would be 16 db for a nonfluctuating target. Second, the decorrelation times of sea clutter were calculated and found to be so small that for side-looking radars sea clutter samples are independent from pulse to pulse but found to be so large for forward-scanning radars that one finally obtains decorrelation from sea motion instead of from platform motion. Third, a fluctuating target was considered, and the losses were calculated and compared with those of a nonfluctuating target. Roughly, one needs 1 to 4 db more power to detect a fluctuating target as opposed to a nonfluctuating target. Then, the ionosphere was considered, and the effects of Faraday rotation and the random phase shift were calculated. Degradation varies from intolerable below 900 MHz to negligible at 3 GHz. Next, some of the aspects of data processing were studied; the optimal integration angle was found, the optimal weighting was calculated, and azimuthal position estimators were considered. Surprisingly, optimal weighting gives a pattern only 0.3 db better than uniform weighting. Finally, a way was determined of using an adaptive threshold and soft limiting to maintain a constant false alarm rate.

PROBLEM STATUS

This is a final report on one phase of the problem; work on other phases continues.

AUTHORIZATION

NRL Problem R02-46
Project A375-38-006/6521, F019-02-01

Manuscript submitted September 13, 1968.

OCEAN SURVEILLANCE STATISTICAL CONSIDERATIONS
(Unclassified Title)

SUMMARY (S)

After the development of ground-based operational naval radars in the 1930's, they were placed on ships and later in aircraft. Now that the space age is here, a logical evolution should include placing a naval radar in a satellite. This report discusses some of the general statistical considerations associated with the detection of targets on the ocean's surface from a satellite-based radar.

In the first section the probability of false alarm, the probability of detection, and the required signal-to-noise ratio for ocean surveillance are discussed. From calculations of the number of false alarms one would obtain per orbit it appears desirable to have a very low false alarm rate, i.e., 10^{-9} to 10^{-10}. Thus, if a probability of detection of 0.99 is desired, an integrated signal-to-noise ratio of about 16 db is necessary for nonfluctuating targets.

In the second section the decorrelation times of the sea clutter due to the radar's platform motion are calculated. The decorrelation times for a side-looking radar are so small that one has independent sea clutter samples from pulse to pulse. However, for a forward-scanning system the decorrelation times are so large that one finally obtains decorrelation from the sea's motion as opposed to the platform's motion.

In the third section a simplified target model consisting of a collection of point scatterers is proposed. Employing this model, a Monte Carlo method is used to calculate the number of independent target returns one receives from this target model as a function of integration time, frequency, and aspect angle. Then, by using Swerling's curves, the required signal-to-noise ratios to obtain a probability of false alarm of 10^{-10} and a probability of detection of 0.9 for fluctuating targets is found as a function of frequency and integration time.

In the fourth section the average daily worst case ionosphere is assumed. From this model, the degradations in the signal-to-noise ratios and degradations in the signal-to-clutter ratios are calculated. All frequencies below 900 MHz have intolerable degradations and so does 900 Mc above 200 naut mi altitude. The degradation disappears swiftly as the frequency is increased; so that, there is essentially no loss at 3 GHz. Also, the ionosphere imparts a random phase shift on the signal which restricts the coherent integration time to the time required for the ionosphere to shift the signal 0.8 radian.

In the fifth section the optimal integration angle is found to vary between 0.92 and 0.88 of the 3-db beamwidth, and the associated scanning loss varies between 1.7 and 1.4 db — the variation being a function of the number of pulses integrated. Then, the optimal weighting pattern is calculated and the surprising result is found that the optimal pattern is only 0.3 db better than the uniform weighting. Finally, several methods are presented for estimating the azimuthal position. These methods give results which are about 20% larger than the smallest theoretical accuracies obtainable.

In the final section a method of using an adaptive threshold and soft-limiting to obtain a constant false alarm rate is presented. The soft-limiting loss is shown to be very small if the limiting level is about the 3σ point of the noise distribution.

SIGNAL-TO-NOISE RATIO (S)

Single-Look Radar (S)

Before one can determine the minimum acceptable signal-to-noise ratio, one must first decide where one should operate on the detection curve for a given S/N ratio; that is, one must find the probability of false alarm P_{fa} and the probability of detection P_d. For example, with a 13-db S/N ratio, one can achieve a $P_{fa} = 10^{-6}$ and $P_d = 0.9$; however, one could also achieve a $P_{fa} = 10^{-5}$ and a corresponding $P_d = 0.8$. To decide which of these two conditions is better, a Bayesian approach can be adopted; that is, a cost function can be generated.

A particular cost function can be based on the argument that if one is trying to track the ships on the ocean, then either missing a target or detecting a false one will cause equal difficulty with the tracking procedure. The optimal operating point (P_{fa}, P_d) can be considered to be the point that maximizes $I(P_{fa}, P_d, S/N)$ for a given S/N ratio, where

$$I(P_{fa}, P_d, S/N) = \text{No. of targets detected} - \text{No. of false alarms}$$

$$P_d \cdot (\text{No. of targets}) - P_{fa} \cdot (\text{No. of decisions})$$

This cost function is usually called the Ideal Observer. Middleton (1) discusses this function further.

To calculate the optimal operating point, particular radar configurations must be assumed so that the number of targets and number of decisions can be calculated. The radar configurations assumed are given in Table 1.

Table 1
Radar Configurations Assumed

Configuration	Swath Width (naut mi)	Resolution (ft)	
		Range	Azimuth
1	800	200	200
2	1000	50	1000
3	1000	50	12,000

For configurations 1 and 2 the number of decisions is 1.5×10^{10} and the number of targets is approximately 600 in a 90-minute interval — a typical orbital time. (The number of decisions is equal to the area put under surveillance per orbit divided by the area of the resolution cell.) Consequently, to find the optimal operating point for each S/N ratio, Table 2 was generated. This table was generated for a nonfluctuating target from curves taken from Ref. 2.

From Table 2, one can easily extract the optimal operating point (the point that maximizes the cost function) for each S/N ratio. The operating points for each S/N ratio are presented in Table 3.

Table 2
Evaluation of the Cost Function (Number of Targets Detected Minus the Number of False Alarms) for Configurations 1 and 2 of Table 1, for which the Number of Targets is 600 and the Number of Decisions is 1.5×10^{10}

Signal-to-Noise Ratio (db)	Probability of a False Alarm	No. of Targets Detected	No. of False Alarms	Cost Function
13	10^{-7}	480	1500	-1020
	10^{-8}	420	150	270
	10^{-9}	330	15	315
	10^{-10}	240	2	238
	10^{-11}	162	0	162
14	10^{-7}	570	1500	-930
	10^{-8}	540	150	390
	10^{-9}	480	15	465
	10^{-10}	420	2	418
	10^{-11}	330	0	330
15	10^{-7}	594	1500	-906
	10^{-8}	588	150	438
	10^{-9}	570	15	555
	10^{-10}	540	2	538
	10^{-11}	480	0	480
16	10^{-7}	600	1500	-900
	10^{-8}	599	150	449
	10^{-9}	597	15	582
	10^{-10}	594	2	592
	10^{-11}	582	0	582
17	10^{-7}	600	1500	-900
	10^{-8}	600	150	450
	10^{-9}	600	15	585
	10^{-10}	600	2	598
	10^{-11}	599	0	599

Table 3
Optimal Operating Points as Taken from Table 2

S/N Ratio (db)	P_{fa}	No. of False Alarms	P_d	No. of Targets Detected
13	10^{-9}	15	.55	330
14	10^{-9}	15	.8	480
15	10^{-9}	15	.95	570
16	10^{-10}	2	.99	594
17	10^{-11}	0	.999	599

Obviously, S/N ratios of 13 and 14 db are not acceptable because of the low probabilities of detection. On the other hand, any S/N ratio above 15 db is acceptable. Since there is some gain in going from 15 to 16 db but very little gain in going from 16 to 17 db, it appears that 16 db is a sufficiently large S/N ratio.

To show that this result is insensitive to the particular system considered, let us consider configuration 3, where the azimuthal resolution is 12,000 ft and the number of decisions has been reduced to 1.2×10^{11}. The cost function for this system is given in Table 4.

Again looking at the optimal operating points, one comes to the previous conclusion; i.e., any S/N ratio greater than 15 db is acceptable. Thus, as long as one has large swath widths and small range resolution cells, an S/N ratio of about 16 db will be required.

Multilook Radars (S)

In the previous paragraphs, the assumption of a single-look radar has been made; however, in this subsection the consequences of the radar being able to look at each resolution cell several times will be investigated. For simplicity, we initially consider a two-look radar, with the time between looks being 90 seconds. (For a target to be detected, it must be detected on both looks.) Now, if targets of interest have a maximum velocity of 30 knots, they can travel 4560 ft in 90 seconds. Consequently, on the second look, the target can appear in any of the following number of resolution cells (a cell is 200 ft by 200 ft) which surround the initial observation of the target:

$$\frac{4560^2}{200 \times 200} \approx 1630 \text{ cells}.$$

If N is the number of false alarms per look, the probability that a false alarm in the first look will be matched with any of the 1630 cells surrounding every false alarm for the second look is approximately

$$\frac{1630\ N}{1.5 \times 10^{13}}.$$

Table 4
Evaluation of the Cost Function for Configuration 3 of Table 1, for which the Number of Targets is 600 and the Number of Decisions is 1.2×10^9

Signal-to-Noise Ratio (db)	Probability of a False Alarm	No. of Targets Detected	No. of False Alarms	Cost Function
13	10^{-7}	480	120	360
	10^{-8}	420	12	408
	10^{-9}	330	1	329
	10^{-10}	240	0	240
	10^{-11}	162	0	162
14	10^{-7}	570	120	450
	10^{-8}	540	12	538
	10^{-9}	480	1	479
	10^{-10}	420	0	420
	10^{-11}	330	0	330
15	10^{-7}	594	120	474
	10^{-8}	588	12	576
	10^{-9}	570	1	569
	10^{-10}	540	0	540
	10^{-11}	480	0	480
16	10^{-7}	600	120	480
	10^{-8}	599	12	587
	10^{-9}	597	1	596
	10^{-10}	594	0	594
	10^{-11}	582	0	582
17	10^{-7}	600	120	480
	10^{-8}	600	12	588
	10^{-9}	600	1	599
	10^{-10}	600	0	600
	10^{-11}	599	0	599

Finally, the total number of false tracks is approximately

$$\frac{1630\ N^2}{1.5\times 10^{10}}\ .$$

If one can tolerate ten false alarms per orbit, the number of false alarms per look, N, is 9560, and the probability of false alarm per look is

$$P_{fa} = \frac{9560}{1.5\times 10^{10}} = 0.6\times 10^{-6}\ .$$

If one requires an overall probability of detection of .98, the probability of detection per look is .99. For $P_{fa} = 0.6\times 10^{-6}$ and $P_d = .99$ the S/N ratio required is about 14.2 db. One can perform a similar analysis allowing one or 100 false alarms instead of ten. Then, the corresponding S/N ratios are 14.5 and 14.0 db respectively. Thus, by using two looks instead of one look, one can pick up only about 1.5 db. The gain is smaller than one would expect because

1. A small change in the S/N ratio causes a large percentage change in P_{fa}.

2. The targets are moving; thus, one has a multitude of ways to match up the possible targets.

By a similar line of reasoning, the number of false tracks NFT (for an M-look radar, with each look separated by 90 seconds) is approximately

$$\mathrm{NFT} = N\left[\frac{1630\ N}{1.5\times 10^{10}}\right]^{M-1}$$

If NFT = 1 and $M = 3$, $N = 43{,}900$ false alarms per look; and the corresponding S/N ratio for a $P_d = 0.993$ is 14.3 db. Thus, a three-look radar is only 0.3 db better than a two-look radar. In fact, the performance will improve very little as the number of looks is increased; for instance, a ten-look radar is only 0.3 db better than a three-look radar.

SEA CLUTTER DECORRELATION TIME (S)

To determine the gain associated with integrating in the presence of sea clutter, a correlation criterion is defined as follows: Since the area of the resolution cell is very large, the returned signal is the resultant of scattering from many scatterers within a single resolution cell; then, two samples from a given resolution cell will be uncorrelated if the maximum change in the one-way range separation of several scatterers exceeds half a wavelength. In the following development, the sea clutter is assumed to be uniformly distributed in a range cell and the decorrelation is assumed to be entirely due to the motion of the radar platform; that is, the sea is assumed to be motionless. At time $t = 0$ (Fig. 1) the ranges to the two scatterers are equal; at time $t = t_c$ the ranges are given by

$$R_1^2 = R^2 + y^2 - 2Ry\cos\theta_1 \qquad (1)$$

and

$$R_2^2 = R^2 + y^2 - 2Ry\cos\theta_2 \qquad (2)$$

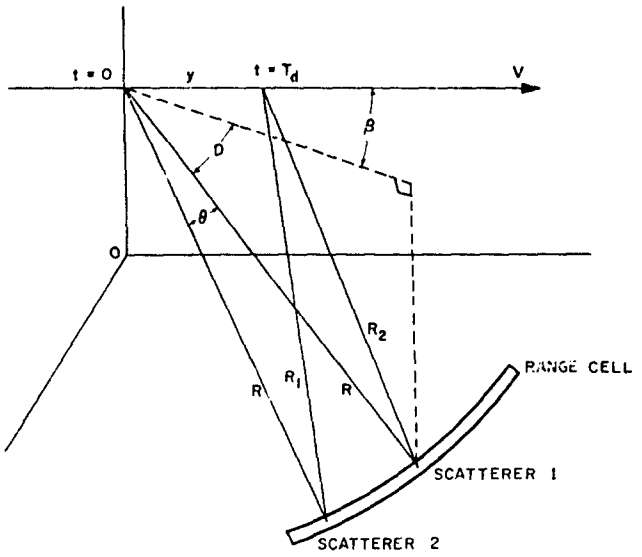

Fig. 1 - Squinted radar configuration

where

$$\cos \quad (\cos D) \cos \qquad (3)$$

and

$$\cos \quad (\cos D) \cos (+ \cos D)$$

in which is the angle between the sight vector and the velocity vector of the radar platform, D is the depression angle, is the squint angle, and 2 is the beamwidth. Subtracting Eq. (2) from Eq. (1) yields

$$R_1^2 - R_2^2 \quad 2Ry (\cos \quad \cos)$$

or

$$y \quad \frac{(R_1 + R_2)(R_1 - R_2)}{2R(\cos \quad \cos)} .$$

One can now make the substitutions

$$R_1 + R_2 \quad 2R$$

and

$$R_1 - R_2 \quad \backslash 2 ,$$

yielding

$$y \quad \frac{1}{2(\cos \quad \cos)} .$$

Finally, letting $\rho = VT_d$ (where V is the velocity of the radar platform) and solving for T_d, one obtains

$$T_d = \frac{\lambda}{2V(\cos\psi - \cos\psi_s)} \quad (4)$$

Note that λ and ρ must have the same distance dimension. Equation (4) was programed for the CDC 3800 computer at NRL, and T_d was calculated as a function of frequency, beamwidth, squint angle, and depression angle. Since the amount of output data is enormous, only two special cases will be presented: the side-looking radar and the forward-scanning radar.

Side-Looking Radar (S)

When the radar is a side-looking radar, the squint angle ψ_s equals 90 degrees. Then Eq. (3) implies ψ = 90 degrees. If one uses the small angle approximation for $\cos\theta$, Eq. (4) reduces to

$$T_d = \frac{\lambda}{2V\theta}$$

Using V = 25,000 ft/sec, T_d was calculated for various beamwidths and frequencies selected from the available radar bands (Table 5). Reviewing the table, one notices that, except for one or two instances, all the returning pulses can be considered independent. Consequently, the integration gain for the sea clutter is the same as for the thermal noise.

Table 5
Decorrelation Time for A Side-Looking Radar

Frequency (MHz)	T_d (sec) for Various Beamwidths			
	0.5	1.0	1.5	2.0
140	0.0322	0.0161	0.0107	0.0081
220	0.0205	0.0102	0.0068	0.0051
440	0.0102	0.0051	0.0034	0.0026
900	0.0050	0.0025	0.0017	0.0013
1300	0.0035	0.0017	0.0012	0.0009
2900	0.0016	0.0008	0.0005	0.0004
5250	0.0009	0.0004	0.0003	0.0002
8500	0.0005	0.0003	0.0002	0.0001

Forward-Scanning Radar (S)

When the radar is a forward-scanning radar, the squint angle ψ_s equals 0 degree. Then Eq. (3) shows that $\psi = \theta$. If one uses the small angle approximation to $\cos\theta$, Eq. (4) reduces to

$$T_c = \frac{\lambda \cos D}{V_c} .$$

Using D = 20 degrees and V = 25,000 ft/sec, T_c was calculated for the beamwidths and frequencies of interest (Table 6). The decorrelation times in Table 6 are quite large. In fact, the decorrelation due to the motion of the sea is less than most of the times in Table 6. This decorrelation time is given by

$$T_c = \frac{\lambda}{2V_s} , \tag{5}$$

where V_s is the sea particle velocity. Using Table 7 (3), for sea state 4, Eq. (5) reduces to

$$T_c = \frac{\lambda}{2.1} ,$$

where λ is the wavelength in meters (f = 30 frequency in megahertz). The decorrelations due to the sea motion for the frequencies of interest are almost the same as those given in Table 6 for a 2-degree beamwidth. Consequently, the 2-degree beamwidth decorrelations should be used for any beamwidths smaller than 2 degrees.

Table 6
Decorrelation Time for A Forward-Scanning Radar

Frequency (MHz)	T_c (sec) for Various Beamwidths			
	0.5	1.0	1.5	2.0
140	13.869	3.467	1.541	0.866
220	8.826	2.206	0.980	0.551
440	4.413	1.103	0.490	0.275
900	2.157	0.539	0.239	0.134
1300	1.493	0.373	0.166	0.093
2900	0.669	0.167	0.074	0.041
5250	0.369	0.092	0.041	0.023
8500	0.228	0.057	0.025	0.014

Since the decorrelation times are still quite large, the integration gain associated with sea clutter will be less than the integration gain associated with the noise. When the sea clutter samples are correlated, the integrated signal-to-clutter plus noise ratio should be calculated as follows: First, the signal (clutter + noise) ratio for one pulse is given by $S/(C+N)$, and the ratio for n pulses is given approximately by

$$\frac{S}{C+N} = \frac{S}{C+N} \, I(n_e) ,$$

where $I(n_e)$ is the integration gain normally associated with n pulses and n_e is the effective number of independent pulses of sea clutter integrated:

Table 7
Waves Generated by a Local Wind at Sea

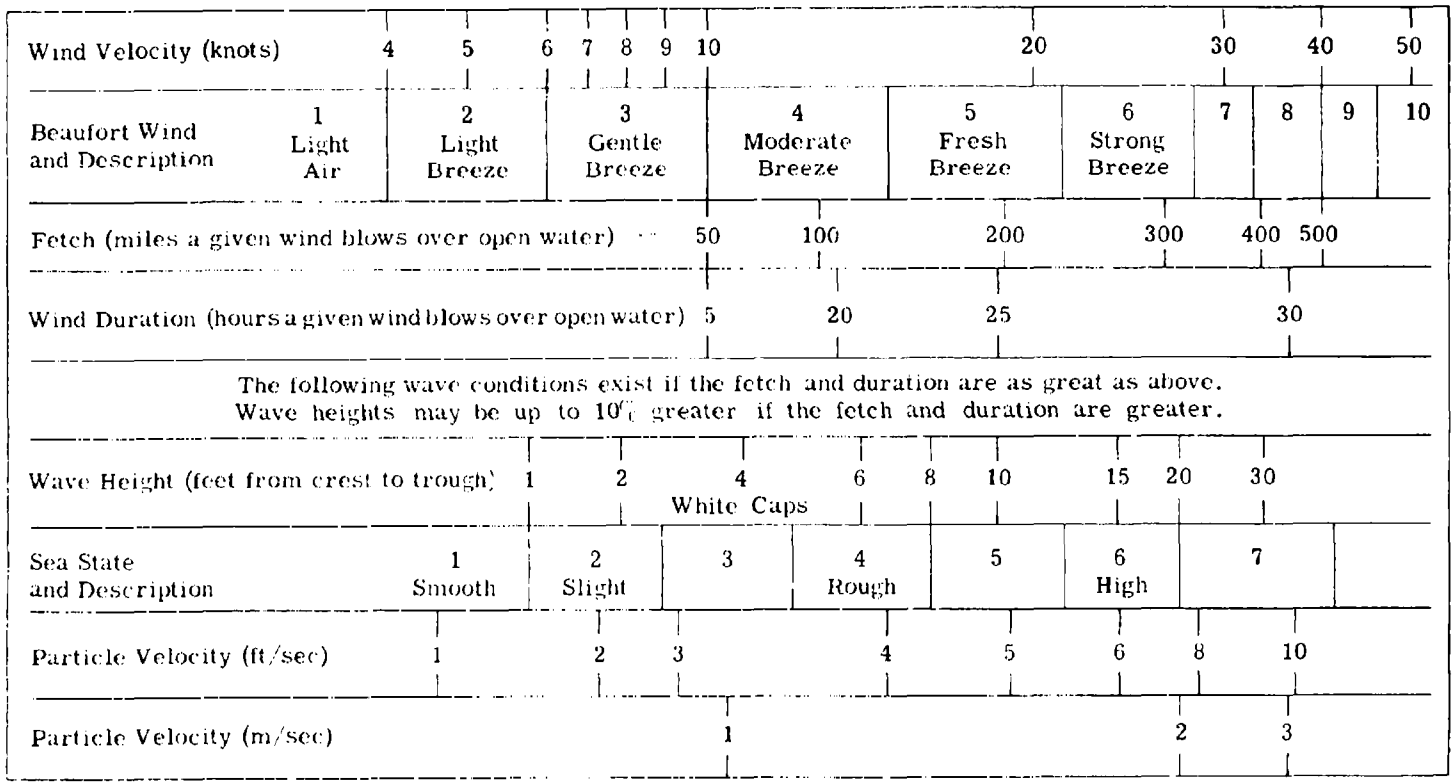

$$M_c = \begin{cases} M, & \text{if } T_c \cdot \text{prf} \leq 1, \\ \dfrac{M}{T_c \cdot \text{prf}}, & \text{if } T_c \cdot \text{prf} \geq 1. \end{cases}$$

The prf is the pulse repetition rate of the radar.

The question remains as to how much one must squint the beam before all the pulses will decorrelate. Since the unambiguous range of a forward-scanning radar requires a prf of about 65, a decorrelation time of about 0.015 second is necessary. Thus, using Table 8, which gives the decorrelation time at a 4-degree squint angle, one can see that

Table 8
Decorrelation Time for a 4-degree Squint Angle

Frequency (MHz)	T_c (sec) for Various Beamwidths			
	0.5°	1.0°	1.5°	2.0°
140	0.446	0.216	0.139	0.101
220	0.284	0.137	0.089	0.064
440	0.142	0.068	0.044	0.032
900	0.069	0.033	0.021	0.015
1300	0.048	0.023	0.015	0.011
2900	0.021	0.014	0.006	0.005
5250	0.011	0.005	0.003	0.002
8500	0.007	0.003	0.002	0.001

one will have complete independence of the clutter samples if one uses any of the following antennas and frequency combinations:

2.0-degree antenna at 900 MHz

1.5-degree antenna at 1300 MHz

1.0-degree antenna at 2900 MHz

0.5-degree antenna at 5250 MHz and 8500 MHz.

Thus, if one has any of the combinations given above, one will have complete independence of clutter outside the 4-degree sector and partial dependence of clutter inside the 4-degree sector.

If the power necessary to detect a given size target along the scanned area were calculated, an exorbitant amount of power would be required in the center section due to the clutter correlation. Thus, to reduce the required power, it seems desirable to slow down the scan rate in the center section so as to obtain more independent clutter samples. If one is completely clutter limited (no thermal noise), an estimate of the slow-down rate can be obtained by dividing the desired decorrelation time (0.015 second) by the decorrelation times of the sea clutter. For instance, at 1300 MHz, Table 6 gives a decorrelation time of 0.093 second. Thus, the slow-down rate should be

$$\frac{0.015}{0.093} = 0.16 \text{ at } 1300 \text{ MHz} \tag{6}$$

and

$$\frac{0.015}{0.041} = 0.37 \text{ at } 2900 \text{ MHz}. \tag{7}$$

Since one is not really clutter limited, the optimal slow-down rates will be larger than those given in Eqs. (6) and (7). In fact, a slow-down rate of 0.5 is probably near the optimum.

TARGET FLUCTUATIONS (U)

Point Scatterers as a Target Model (U)

Most targets can be considered to consist of many individual point scatterers. If one would look at the target from different aspect angles, the target's cross section would appear to fluctuate because of the cancellations and reinforcements between the different scatterers.

To determine what the target model should be, an approach similar to one used in calculating the sea clutter decorrelation time was adopted. First, from the geometry (Fig. 2) one can write

$$\Delta y = l \cos \alpha,$$

$$\Delta x = l \sin \alpha,$$

$$R^2 = y^2 + x^2, \tag{8}$$

$$(R + \Delta R)^2 = (y + \Delta y)^2 + (x + \Delta x)^2. \tag{9}$$

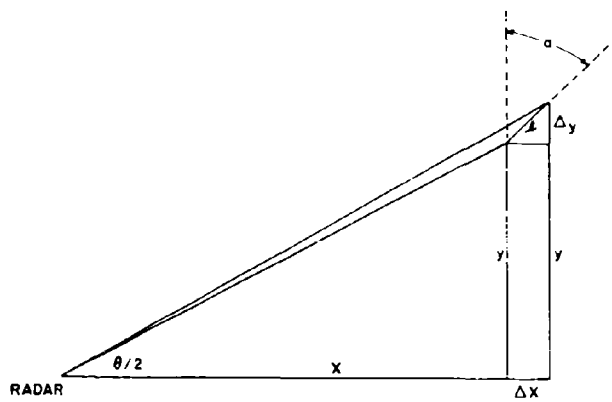

Fig. 2 - Radar geometry for target fluctuations, with the target of length l shown at one extreme of the beamwidth.

Subtracting Eq. (8) from Eq. (9) one obtains

$$2R\Delta R + \Delta R^2 = 2y\Delta y + \Delta y^2 + 2x\Delta x + \Delta x^2 .$$

Consequently, the one-way range difference is approximately

$$\Delta R \approx (y\Delta y + x\Delta x)/R ,$$

and the two-way phase change is

$$\Delta\phi = \frac{2\pi}{\lambda}(2\Delta R) = \frac{4\pi}{\lambda R}(y\Delta y + x\Delta x),$$

where λ is the radar wavelength. Usually, the number of independent samples as the beam sweeps past the target is taken to be equal to the number of 2π phase shifts across the beam. At one extreme of the beam, $y = R\theta/2$ and

$$\Delta\phi = \frac{4\pi}{\lambda R}(R\theta\Delta y/2 + x\Delta x). \tag{10}$$

At the other extreme, $y = -R\theta/2$ and

$$\Delta\phi = \frac{4\pi}{\lambda R}(-R\theta\Delta y/2 + x\Delta x). \tag{11}$$

Subtracting Eq. (11) from Eq. (10), dividing by 2π, and adding unity yields the number of independent samples:

$$\text{Indep.} = \frac{2\theta\Delta y}{\lambda} + 1 . \tag{12}$$

The returning signal from N equal scatterers is

$$S = \sum_{i=1}^{N} \sin(\omega t + \phi_i)$$

or, equivalently,

$$S = \sin\omega t \sum_{i=1}^{N} \cos\phi_i + \cos\omega t \sum_{i=1}^{N} \sin\phi_i ,$$

and the cross section of the target σ is proportional to

$$\sigma \propto \left(\sum_{i=1}^{N} \cos\phi_i\right)^2 + \left(\sum_{i=1}^{N} \sin\phi_i\right)^2 \tag{13}$$

While the target passes through the beam, the target will appear to fluctuate because of the changing phases. Typical fluctuations are shown in Fig. 3 for two target orientations. For the θ = 0.0-radian case, Eq. (12) indicates the presence of only 2.7 independent samples; and for the θ = 1.0 case, Eq. (12) indicates 1.9 independent samples. If one would use the common method of block correlation with this number of independent samples, there would exist a probability of obtaining a very low strength signal requiring a

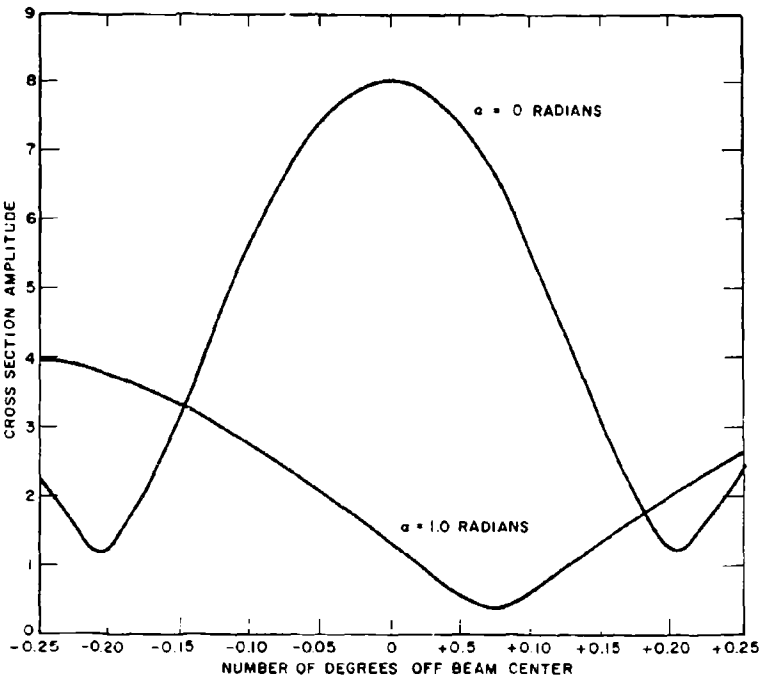

Fig. 3 - Returned signal from a fluctuating target (ℓ = 100 ft; λ = 1.0 ft; N = 8; α = 0.5 degree)

very high transmitted power to detect it. However, if one took a very large number of samples (large in relation to the number of independent samples), one would essentially obtain the average returning signal over the given aspect angle; and it appears from Fig. 3 that because of the correlation between samples one will not obtain the small cross sections possible when using block correlation in connection with Eq. (12). To test this conjecture, the following experiment was conducted: For each of 100 cases, eight scatterers were uniformly distributed over a length of 100 feet oriented at an angle of α = 0.0 radians. For each distribution, the average returning signal S_i was found. Then, the average and standard deviation of the 100 $\{S_i\}$ were calculated:

$$E\{S_i\} = 2.5$$

and (14)

$$\{\mathrm{var}\{S_i\}\}^{1/2} = 0.65 .$$

Since what one is really trying to do with block correlation and independent samples is to model the actual situation, what one wants to find is the number of independent samples necessary to approximate the actual distribution — or equivalently in this case, the standard deviation. To accomplish this, in the beginning 100 random samples were taken from the 100 configurations, and 100 averages $\bar{X}$ each consisting of only one point were found. Then, the standard deviation of the 100 $\{\bar{X}_i\}$ was calculated:

$$\{\mathrm{var}\{\bar{X}_i\}\}^{1/2} = 1.12 .$$

Since 1.42 is greater than the true standard deviation, more than one independent sample exists. To find the exact number, the above procedure was repeated. However, this time, each X_i consisted of two, three, and four independent samples. The standard deviations of these cases are as follows:

X_i consists of two samples, $[\mathrm{var}(X_i)]^{1/2} = 0.98$, (15a)

X_i consists of three samples, $[\mathrm{var}(X_i)]^{1/2} = 0.78$, (15b)

X_i consists of four samples, $[\mathrm{var}(X_i)]^{1/2} = 0.61$. (15c)

Thus, comparing Eqs. (15) to Eq. (14) it appears that there are approximately four independent samples present compared with the 2.7 indicated by Eq. (12). Repeating this procedure several other times always yielded the same result — the number of independent samples required to equate the standard deviations was always slightly larger than the number given by Eq. (12).

In the rest of this section, the number of independent samples will be defined to be that number for which the standard deviations of X_i and s_i are equal. Before proceeding to calculate the number of independent samples as a function of aspect angle, the problem will be reformulated to include ship roll.

Reformulation to Include Ship Roll (U)

The coordinate systems for the radar platform and for the target are shown in Fig. 4. The following notation and definitions will be used:

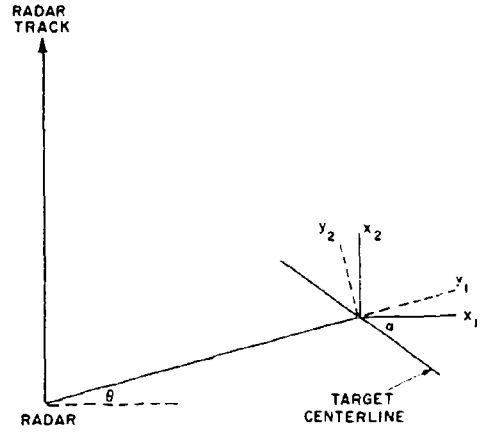

Fig. 4 - Radar and target coordinate systems

x_1 axis which is the line on the earth's surface perpendicular to the radar track,

x_2 axis which is the line on the earth's surface parallel to the radar track,

x_3 axis which completes the right-handed coordinate system,

y_1 axis which is the line from the radar to the target,

y_2 axis which is perpendicular to y_1 and lying in the $x_1 x_2$ plane,

y_3 axis which completes the right-handed coordinate system,

squint angle of the radar, i.e., the angle from the radar to the target center measured with respect to the x_1 axis in the $x_1 x_2$ plane,

angle the center line of the target makes with the x_1 axis,

roll angle of the target,

grazing angle.

Let us initially assume the target is aligned along the x_1 axis ($\psi = 0$) and the problem is to find the coordinates of a point in the y system whose coordinates in the x system are a_1, a_2, and a_3. First, the new coordinates due to a roll angle are given by

$$\begin{bmatrix} b_1 \\ b_2 \\ b_3 \end{bmatrix} = \begin{bmatrix} 1 & 0 & 0 \\ 0 & \cos & -\sin \\ 0 & \sin & \cos \end{bmatrix} \begin{bmatrix} a_1 \\ a_2 \\ a_3 \end{bmatrix}. \tag{16}$$

To line up the x_2 and y_2 axes and to compensate for the fact that the target is not aligned along the x_1 axis, it is necessary to rotate about the x_1 axis an angle of (-):

$$\begin{bmatrix} c_1 \\ c_2 \\ c_3 \end{bmatrix} = \begin{bmatrix} \cos(\quad - \quad) & -\sin(\quad - \quad) & 0 \\ \sin(\quad - \quad) & \cos(\quad - \quad) & 0 \\ 0 & 0 & 1 \end{bmatrix} \begin{bmatrix} b_1 \\ b_2 \\ b_3 \end{bmatrix}. \tag{17}$$

Finally, one needs to rotate through the grazing angle :

$$\begin{bmatrix} d_1 \\ d_2 \\ d_3 \end{bmatrix} = \begin{bmatrix} \cos & 0 & -\sin \\ 0 & 1 & 0 \\ \sin & 0 & \cos \end{bmatrix} \begin{bmatrix} c_1 \\ c_2 \\ c_3 \end{bmatrix}. \tag{18}$$

Points with the same x_1 coordinate are at essentially the same range. Hence, the relative phase change with respect to the center of the target is given by

$$\phi = \frac{4\pi}{\lambda} d_1 \tag{19}$$

Substituting Eqs. (16), (17), and (18) into Eq. (19) yields

$$\phi = \frac{4\pi}{\lambda} \left[a_1 \cos(\quad - \quad) \cos \right. \\ \left. - a_2 \cos \sin(\quad - \quad) \cos + \sin \sin \right. \\ \left. + a_3 \sin \sin(\quad - \quad) \cos - \cos \sin \right]. \tag{20}$$

Next, Eqs. (13) and (20) were used in a Monte Carlo investigation to determine the number of independent samples for side-looking and forward-scanning systems as a function of the orientation of the target. In lieu of the absence of a standardized ship model, the following ship parameters, which do not seem unreasonable, were used:

Length of target, 150 feet,

Width of target, 20 feet,

Height of target, 15 feet,

Roll angle ϕ, $\phi_{max} \sin(2\pi f_p t - \phi_0)$,

ϕ_{max}, 0.2 radian,

T_p, 10 seconds.

Also, the following radar parameters were used:

Beamwidth, 0.5 degree,

Grazing angle, 3.5 degrees,

Integration time, 1.5 sec for a forward-scanning system,
3.2 sec for a side-looking system.

For each of the 100 configurations used, 14 scatterers were uniformly distributed in the rectangular target volume, and the initial phase of the roll ϕ was uniformly distributed on 0 to 2π. The number of independent samples for the side-looking radar is shown in Fig. 5 and the number of independent samples for the forward-scanning radar is shown in Fig. 6. For the side-looking radar, the number of independent samples increases from one to 24 as the target orientation changes from bow to broadside; and for the forward-scanning radar the variation is one to 11 from bow to broadside. To see how much these fluctuations cost with respect to complete independence between pulses, one can consult Table 9, which was derived from Swerling's report (4) about log-normal fluctuating targets.

Table 9
Required Increase in the S/N Ratio with Respect to Complete Independence*

Probability of Detection, P_d	S/N Ratio Increase for Decreasing Numbers of Independent Samples (db)				
	100	10	4	2	1
.99	0	2	4.75	7.25	11.75
.9	0	1.25	3	4.5	7.5

*These figures are for a mean-to-median ratio of 2. Also, as one can see from Guargaglini (5) these numbers can be used for a Rayleigh fluctuating target.

If one wanted to maintain a probability of detection of .99 for all target orientations, it would be necessary to increase the S/N ratio by either 7.25 or 11.75 db, depending on the operating frequency. This seems like an exorbitant waste of power which is not justified because of the following discussion.

Even though the probability of detection is greatly deteriorated at bow aspects, it is very little deteriorated at broadside. A natural question to ask is what is the overall probability of detection assuming that ships will be uniformly distributed in aspect. By using Swerling's curve (Fig. 7) and Fig. 5, a side-looking radar operating at = 0.333 feet has the following minimum probabilities of detection:

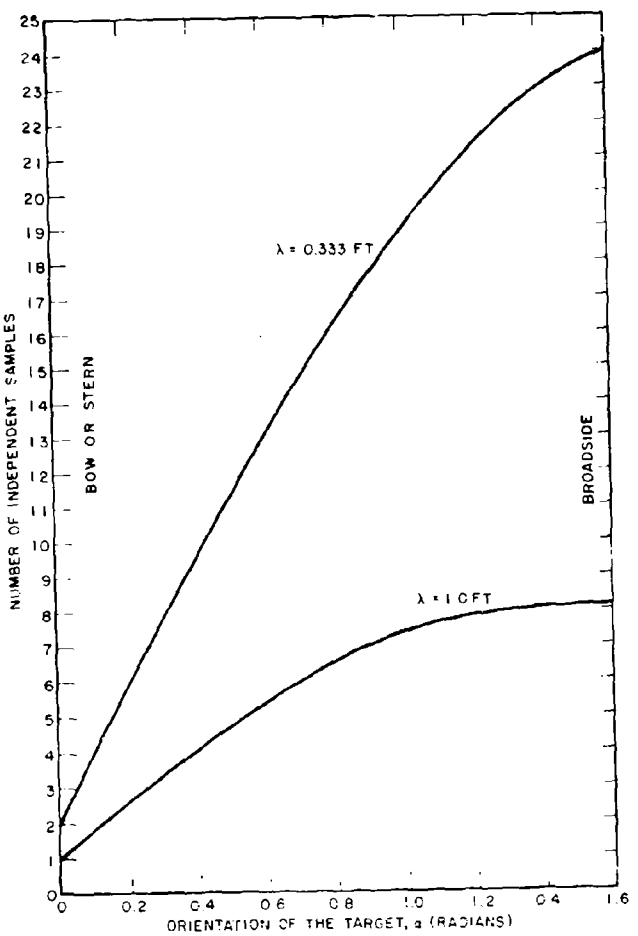

Fig. 5 - The number of independent samples for a side-looking radar (grazing angle = 3.6 degrees; integration time = 3.2 sec)

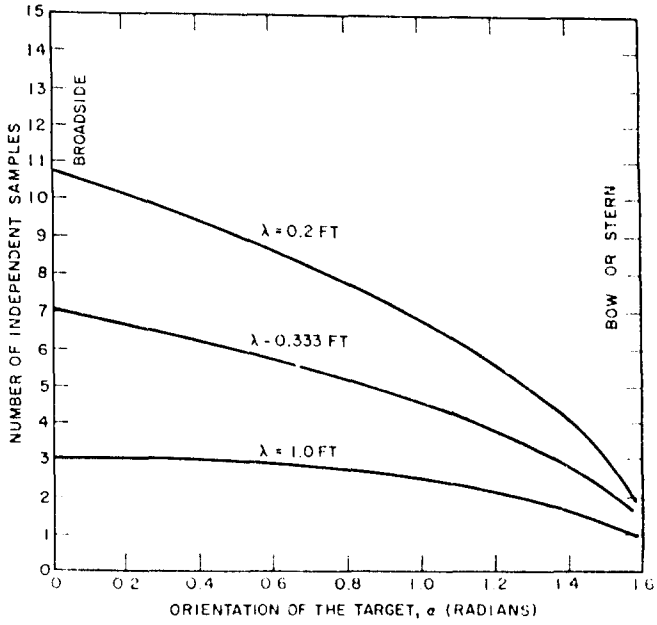

Fig. 6 - The number of independent samples for a forward-looking radar (grazing angle = 3.6 degrees; integration time = 1.5 sec)

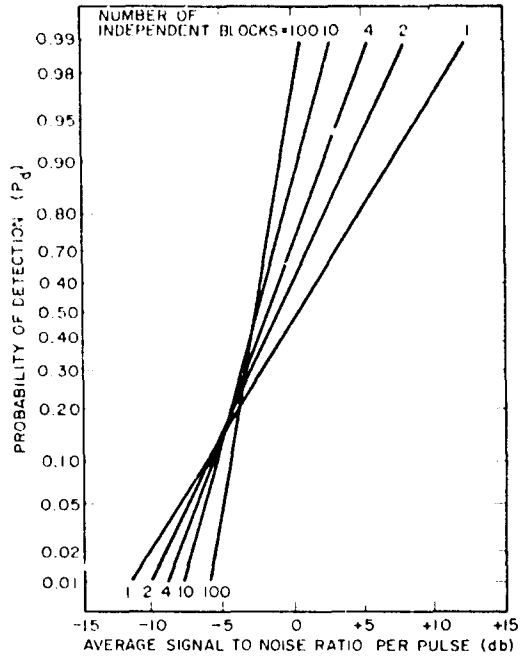

Fig. 7 - Radar detection probability for log-normally distributed targets (= 2; N = 100; probability of a false alarm $P_{fa} = 10^{-7}$)

$$0.0 \leq \alpha \leq 0.1, \qquad \min(P_d) = 0.64,$$

$$0.1 \leq \alpha \leq 0.4, \qquad \min(P_d) = 0.76,$$

$$0.4 \leq \alpha \leq 2, \qquad \min(P_d) = 0.90.$$

Hence, the overall probability of detection is

$$P_d = \frac{2}{5}[0.1(0.64) + 0.3(0.76) + (2-0.4)(0.9)] = 0.856.$$

The calculation was performed for various integrated S/N ratios, frequencies, and the two radar configurations. The results are shown in Table 10.

Table 10
Probability of Detection for Fluctuating Targets*

Integrated S/N Ratio (db)	P_d				
	Side-Looking Radar		Forward-Scanning Radar		
	λ = 1 ft	λ = 0.33 ft	λ = 1 ft	λ = 0.33 ft	λ = 0.2 ft
16	.72	.86	.62	.73	.76
17	.81	.91	.72	.82	.85
18	.88	.96	.80	.89	.91
19	.92	.98	.86	.93	.95
20	.95	.99	.91	.96	.97

*An integrated S/N ratio of 16 db corresponds to probability of false alarm of 10^{-10} and a probability of detection of .99 for the case where all the samples are independent.

Using linear interpolation on Table 10, the following S/N ratios are required for a probability of detection of .9 for fluctuating targets and a probability of false alarm of 10^{-10}. For a side-looking radar

$$S/N = 16.6 \text{ db for } \lambda = 0.33 \text{ ft}, \tag{21a}$$

$$S/N = 18.5 \text{ db for } \lambda = 1.0 \text{ ft}. \tag{21b}$$

For a forward-scanning radar

$$S/N = 17.8 \text{ db for } \lambda = 0.2 \text{ ft}, \tag{21c}$$

$$S/N = 18.2 \text{ db for } \lambda = 0.33 \text{ ft}, \tag{21d}$$

$$S/N = 19.9 \text{ db for } \lambda = 1.0 \text{ ft}. \tag{21e}$$

Thus, with the integrated S/N ratios shown in Eqs. (21), one obtains a probability of detection of over .9 for fluctuating targets and a probability of detection of over .99 for nonfluctuating targets.

The S/N ratios in Eqs. (21) are those required when the target is seen at a grazing angle of 3.5 degrees for 3.2 sec. If the grazing angle is increased, the decorrelation times due to rolling will change, and new S/N ratios will be required. If the grazing angle is increased to 51 degrees with a corresponding integration time of 0.44 sec, the number of independent samples for a side-looking radar is shown in Fig. 8. Comparing Figs. 5 and 8, one sees that one has more independent samples at bow aspect but less independent samples at broadside for the larger grazing angle. Using the same philosophy as before, the probabilities of detection have been recalculated for the larger grazing angle and are shown in Table 11. The values in Table 11 were calculated using Fig. 9 instead of Fig. 7, because at the large grazing angles (small ranges) one is integrating only 29 pulses in comparison with over 100 at the large ranges.

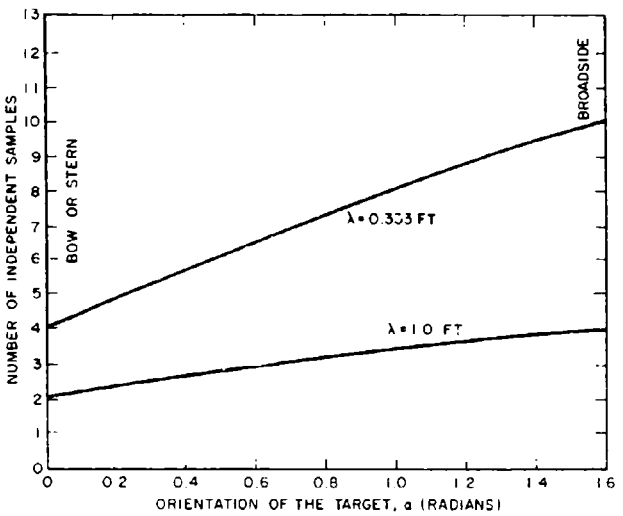

Fig. 8 - The number of independent samples for a side-looking radar (grazing angle = 51 degrees; integration time = 0.44 sec)

Table 11
Probability of Detection for Fluctuating Targets (Grazing angle = 51 degrees; Integration Time = 0.4 sec; Side-Looking Radar)

Integrated S/N Ratio (db)	P_d		Integrated S/N Ratio (db)	P_d	
	λ = 1 ft	λ = 0.33 ft		λ = 1 ft	λ = 0.33 ft
16	.80	.88	18	.91	.96
17	.86	.92	19	.94	.98

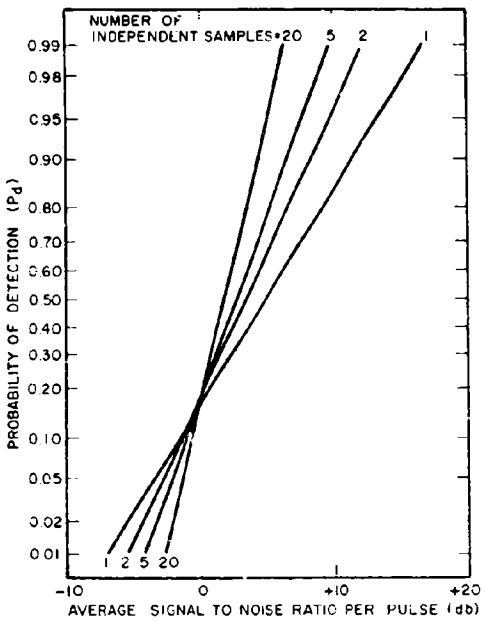

Fig. 9 - Radar detection probability for log-normally distributed targets (σ = 2, N = 20; probability of a false alarm $P_{fa} = 10^{-6}$)

Again using linear interpolation on Table 11, the S/N ratios required for a probability of detection of .9 and a probability of false alarm of 10^{-10} with a grazing angle of 51 degrees and an integration time of 0.44 sec for a side-looking radar are

S/N = 16.5 dB for [illegible] ft. (22a)

S/N = 17.8 dB for [illegible] ft. (22b)

As one can see, these values are slightly smaller than those given in Eqs. (21). Since the values in Eqs. (22) were calculated using Fig. 9, which assumes 20 pulses integrated whereas really 29 pulses are integrated, the required S/N ratios will be slightly larger than those given in Eqs. (22). Consequently, the desired S/N ratio can be considered a constant over all grazing angles.

The required S/N ratios have been calculated for several other integration times. The results of the various calculations are presented in Figs. 10, 11, and 12.

IONOSPHERIC EFFECTS (U)

This section discusses how the ionosphere affects detection of targets at sea. The two major problems caused by passage of the signal through the ionosphere are the Faraday rotation of the signal and the random phase shift associated with the received signal. The approach consists of postulating a very simplified model of these effects and then calculating the degradation caused by these effects.

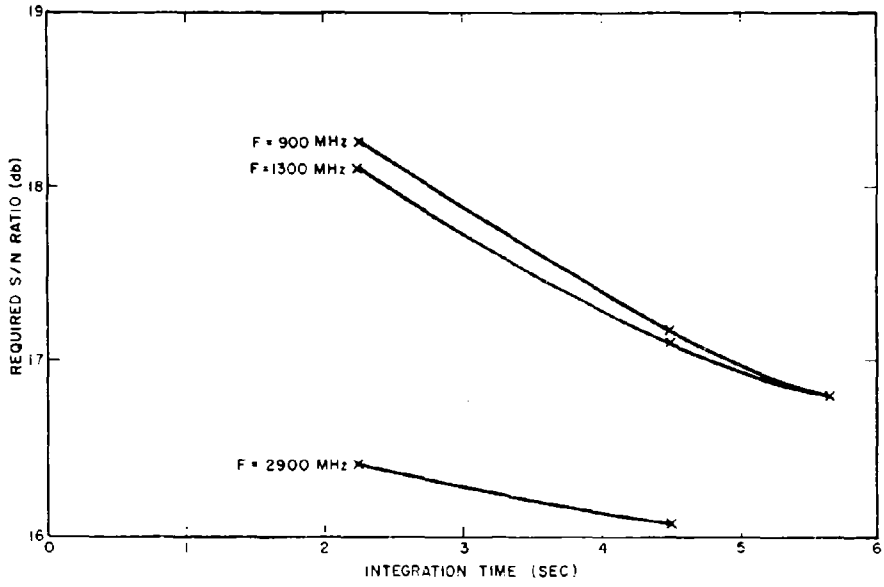

Fig. 10 - Effect of the integration time on the required S/N ratio for a side-looking radar (grazing angle = 3.5 degrees)

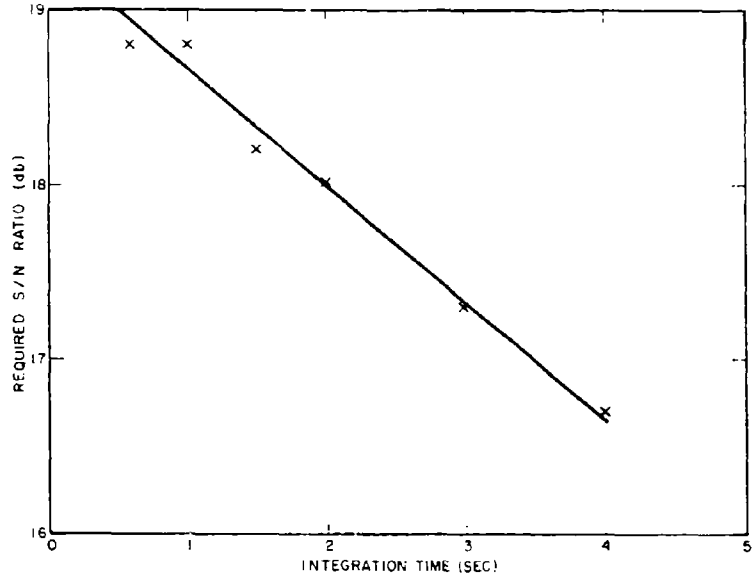

Fig. 11 - Effect of the integration time on the required S/N ratio for a forward-scanning radar (frequency = 2900 Mc; grazing angle = 2 degrees)

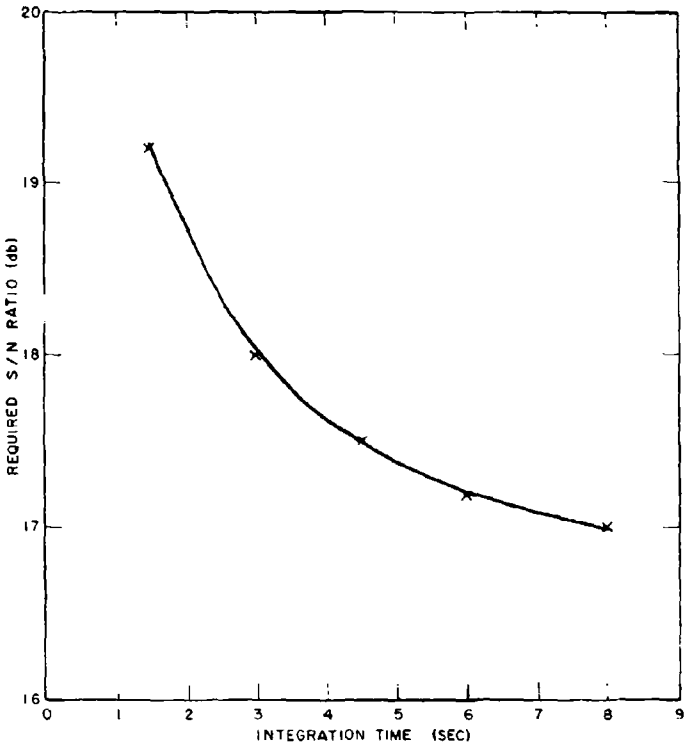

Fig. 12 - Effect of the integration time on the required S/N ratio for a forward-scanning radar (frequency = 1300 Mc; grazing angle = 2 degrees)

Faraday Rotation (U)

Faraday rotation is a complicated function of geographical position, time of day, time of year, orientation of the radar beam with respect to the earth's magnetic field, and many other factors. Therefore, instead of forming an extremely complicated model for Faraday rotation, the postulated model will only reflect some of the worst conditions to be encountered: upper midlatitudes, noon wintertime, 20-degree depression angle, and orientation parallel to the earth's magnetic field. For these conditions, by assuming a Chapman distribution as a model for the ionosphere electron density distribution, the Faraday rotation can be approximated (6) by the following equation and table:

$$\Omega = 2.22 \times 10^{4} \, G_H C_H f^{-2} , \tag{23}$$

Altitude // (naut mi)	G_H	C_H	Altitude // (naut mi)	G_H	C_H
150	1.0	109	300	0.945	322
200	0.97	198	400	0.92	377
250	0.956	272	600	0.91	413

where ϕ is the one-way Faraday rotation in radians, f is the frequency in hertz, G_H is related to the strength of the magnetic field and is a function of the altitude H, and C_H is a slab thickness parameter and is a function of the altitude H. Using Eq. (23) and the table, the one-way Faraday rotations were calculated and are shown in Table 12.

Table 12
One-Way Faraday Rotation of the Signals at Various Frequencies With the Satellite at Various Heights

Altitude H (naut mi)	Faraday Rotation ϕ (radians)							
	140 MHz	220 MHz	440 MHz	900 MHz	1300 MHz	2950 MHz	5250 MHz	8500 MHz
150	12.3	5.0	1.25	0.30	0.14	0.03	0.01	0.00
200	21.7	8.78	2.20	0.53	0.25	0.05	0.02	0.01
250	29.4	11.9	2.98	0.71	0.34	0.07	0.02	0.01
300	34.4	13.9	3.49	0.83	0.40	0.08	0.02	0.01
400	39.2	15.9	3.96	0.95	0.46	0.09	0.03	0.01
600	42.5	17.2	4.30	1.03	0.49	0.10	0.03	0.01

To calculate the degradation in the signal-to-clutter ratio and S/N ratio, it is necessary to calculate the received signal after it has passed through the ionosphere, been reflected at the sea surface, and again passed through the ionosphere. First of all, let us assume that the transmitted electric field is

$$\bar{E}_T = E_1(\hat{H} + g\hat{V}) e^{j(\omega t - kz)}$$

$$= E_1(\hat{H} + g\hat{V}) ,$$

where g is the cross-polarization gain of the antenna and $\hat{H}$ and $\hat{V}$ are unit vectors in the horizontal and vertical directions. Then, the electric field reflected by the sea is given by

$$\bar{E}_s = E_1 \sqrt{\sigma_H} (\cos\theta + g\sin\theta)\hat{H} + e^{j\delta}\sqrt{\sigma_V}(\sin\theta + g\cos\theta)\hat{V} , \quad (24)$$

where σ_H is the sea clutter cross section for horizontal polarization, σ_V is the sea clutter cross section for vertical polarization, ϕ is the one-way Faraday rotation, δ is the phase shift between the horizontal and vertical components that is caused by the reflection, and θ is the incident angle between the horizontal component of E_1 and the sea when there is no Faraday rotation. In reality, θ is a random variable caused by the roughness of the sea. Since its distribution is unknown and since it is not of prime importance in this discussion, we will assume $\theta = 0$. Then Eq. (24) reduces to

$$\bar{E}_s = E_1\left[\sqrt{\sigma_H}(\cos\phi - g\sin\phi)\hat{H} + e^{j\delta}\sqrt{\sigma_V}(\sin\phi + g\cos\phi)\hat{V}\right].$$

The power received by an antenna is proportional to the square of the absolute value of the received electric field. That is

$$P = E_1^2 \sigma_H \left[(\cos^2\psi - g^2 \sin^2\psi) + \sqrt{\frac{\sigma_V}{\sigma_H}} e^{j\phi} (-\sin^2\psi + g^2 \cos^2\psi) \right]$$

$$\times \left[(\cos^2\psi - g^2 \sin^2\psi) + \sqrt{\frac{\sigma_V}{\sigma_H}} e^{-j\phi} (-\sin^2\psi + g^2 \cos^2\psi) \right] \quad (25)$$

represents the backscatter from sea clutter. On the basis of work by Macdonald (7,8) a σ_V/σ_H ratio of 10 db was selected as a good average. Also, it is fairly easy to build a linearly polarized antenna whose cross-polarization response is down at least 20 db ($g = 0.1$). Finally, while ψ varies over a wide range of values, $\psi = 0$ was chosen, since this value yields the worst losses. For these values Eq. (25) gives for the backscatter power from sea clutter

$$C = E_1^2 \sigma_H \left[(\cos^2\psi - 0.01 \sin^2\psi) + 3.16 (-\sin^2\psi + 0.01 \cos^2\psi) \right]^2 \quad (26)$$

A similar approach can be used to find the returning signal power; the only difference is that the ratio σ_V/σ_H of the target cross sections for vertical and horizontal polarizations (again based on Refs. 7 and 8) is -4 db. Thus, the returned signal power is

$$S = E_1^2 \sigma_H \left[(\cos^2\psi - 0.01 \sin^2\psi) + 0.63 (-\sin^2\psi + 0.01 \cos^2\psi) \right]^2 \quad (27)$$

The bracketed term in Eq. (27) represents the degradation of the S/N ratio, and the ratio of Eq. (27) and Eq. (26) represents the degradation of the signal-to-clutter ratio. These losses are presented in Table 13.

Table 13
Degradation of the S/N Ratio and Degradation in the Signal-to-Clutter Ratio Caused by Faraday Rotation

Altitude H (naut mi)	Degradation Factors at Various Frequencies							
	140 MHz	220 MHz	440 MHz	900 MHz	1300 MHz	2950 MHz	5250 MHz	8500 MHz
Signal-to-Noise Power Degradation Factor (Factor in Eq. (27))								
150	0.0001	0.0001	0.0001	0.743	0.974	1.0	1.0	1.0
200	0.0001	0.0001	0.0001	0.340	0.810	0.992	0.998	1.0
250	0.0001	0.0001	0.0001	0.094	0.670	0.986	0.998	1.0
300	0.0001	0.0001	0.0001	0.0120	0.566	0.980	0.998	1.0
400	0.0001	0.0001	0.0001	0.0001	0.460	0.973	0.997	1.0
600	0.0001	0.0001	0.0001	0.0001	0.408	0.967	0.997	1.0
Signal-to-Clutter Degradation Factor (Ratio of Eq. (27) and Eq. (26))								
150	0.0001	0.0001	0.0001	1.0	1.0	1.0	1.0	1.0
200	0.0001	0.0001	0.0001	1.0	1.0	1.0	1.0	1.0
250	0.0001	0.0001	0.0001	0.1632	1.0	1.0	1.0	1.0
300	0.0001	0.0001	0.0001	0.0077	1.0	1.0	1.0	1.0
400	0.0001	0.0001	0.0001	0.0001	1.0	1.0	1.0	1.0
600	0.0001	0.0001	0.0001	0.0001	1.0	1.0	1.0	1.0

In deriving Table 13 the following method was used: For a given frequency and altitude, the losses recorded in Table 13 correspond to the maximum losses associated with any rotation between zero and the maximum Faraday rotation that is given in Table 12. This is why the maximum loss of 0.0001 is so frequent. Also, for small rotations the ratio of Eqs. (27) and (26) is greater than 1, since no depolarization has been assumed; i.e., [illegible]. Consequently, a conservative approach was taken by replacing these gains by 1's.

It seems likely that one could reduce the losses for the low frequencies if one would use circular polarization. This is equivalent to assuming that [illegible]. Then, Eqs. (26) and (27) reduce to

$$C = E_T^2 \, [\text{illegible}] \left[\frac{1}{2} \left(1 - \sqrt{[\text{illegible}]} \right)^2 \right] = 2.31 \, E_T^2 \, [\text{illegible}]$$

and

$$S = E_T^2 \, [\text{illegible}] \left[\frac{1}{2} \left(1 - \sqrt{[\text{illegible}]} \right)^2 \right] = 0.068 \, E_T^2 \, [\text{illegible}]$$

Thus, the S/N power degradation factor is 0.068 and the signal-to-clutter power degradation factor is 0.0297 for circular polarization, these factors being independent of the Faraday rotation.

Random Phase Shift (U)

Another effect of the ionosphere is the random phase shift introduced by variations in the ion density. This phase shift, whose mean is directly proportional to time, limits the coherent integration time. Consequently, the question arises as to how many pulses N one should integrate coherently if one receives [illegible] pulses in time T. Before calculating the optimal coherent integration gain when the mean phase of the received signal drifts linearly with time, the total integration gain will be calculated. First, the received energy for N pulses is given by the correlation

$$E = \sum^{N-1} \int [\text{illegible}] \cos [\text{illegible}] \cos [\text{illegible}] \, dt \qquad (28)$$

where T_p is the time between pulses = 1/prf, [illegible] is the pulse width, and [illegible] is the random phase shift, which will be approximated by its mean; that is [illegible], where [illegible] is the phase shift per unit time and therefore is a function of the frequency [illegible]. Integrating Eq. (28) yields

$$E = \sum^{N-1} \left[\frac{\sin [\text{illegible}]}{2 [\text{illegible}]} - \frac{\sin [\text{illegible}]}{2 \cdot 2 [\text{illegible}]} \right] [\text{illegible}] \qquad (29)$$

which for the [illegible]'s of interest can be approximated by

$$E = \sum^{N-1} \left[[\text{illegible}] \, T_p [\text{illegible}] - \frac{\sin [\text{illegible}] \, T_p}{2 [\text{illegible}]} \right] [\text{illegible}] \qquad (30)$$

Expanding Eq. (30),

$$E = \sum_{i=0}^{N-1} \left[\frac{\sin \omega T_p \cos \omega_c + \cos \omega T_p \sin \omega_c - \sin \omega_c T_p}{2} \right], \tag{31}$$

and substituting the small angle approximations

$$\cos \omega_c \approx 1$$

$$\sin \omega_c \approx \omega_c$$

into Eq. (31), one obtains

$$E \approx \frac{1}{2} \sum_{i=0}^{N-1} \cos \omega T_p . \tag{32}$$

It can be shown that the summation in Eq. (32) can be rewritten as

$$E = \frac{1}{2} \left[\frac{1}{2} + \frac{\sin \left(N - \frac{1}{2} \right) \omega T_p}{2 \sin \omega T_p / 2} \right],$$

which if one uses the small angle approximation reduces to

$$E = \frac{1}{2} \left[\frac{1}{2} + \frac{\sin \left(N - \frac{1}{2} \right) \omega T_p}{\omega T_p} \right]$$

or

$$E = \frac{1}{2} \left[\frac{1}{2} + \left(N - \frac{1}{2} \right) \frac{\sin \left(N - \frac{1}{2} \right) \omega T_p}{\left(N - \frac{1}{2} \right) \omega T_p} \right].$$

If N is large, this can simply be approximated by

$$E \approx \frac{1}{2} \left(N \frac{\sin \Phi}{\Phi} \right), \tag{33}$$

where Φ is the phase shift encountered in time $T_p (N - 1/2)$:

$$\Phi = \omega T_p \left(N - \frac{1}{2} \right).$$

The term in parentheses in Eq. (33) represents the coherent integration gain for N pulses:

$$G = \frac{N \sin \Phi}{\Phi}.$$

Thus, of the M pulses one receives, N consecutive pulses are coherently integrated; and then, the results of these coherent integrations are combined by performing a noncoherent integration on $K = M/N$ pulses. The noncoherent integration gain is given by

$$S(K) = 1 \quad \text{for} \quad K = 1, \tag{34a}$$

$$S(K) = 1.010\,K^{0.944} \quad \text{for} \quad 1 < K < 4, \tag{34b}$$

$$S(K) = 1.282\,K^{0.775} \quad \text{for} \quad 4 \leq K < 20, \tag{34c}$$

$$S(K) = 1.675\,K^{0.685} \quad \text{for} \quad 20 \leq K < 100, \tag{34d}$$

$$S(K) = 2.594\,K^{0.593} \quad \text{for} \quad K > 100, \tag{34e}$$

which are curves that Fox (9) has used to approximate the noncoherent integration gain given in Skolnik (10). Therefore, the gain associated with integrating M pulses, N pulses coherently, is

$$G = \left(N \frac{\sin \Phi}{\Phi}\right) S(M/N), \tag{35}$$

where

$$\Phi = \pi T_p \left(N - \frac{1}{2}\right).$$

The problem of finding the optimal integration time, or equivalently N, is reduced to finding the value of N that maximizes the gain given in Eq. (35). Setting the derivative of Eq. (35) to zero yields a very complicated equation for the optimal value of N. However, if one makes the approximation

$$\Phi \approx \pi T_p N,$$

the equation for the optimal N is quite simple. First, G is then of the form

$$G = \frac{\sin \pi T_p N}{\pi T_p} \frac{A^R M^R}{N^R}.$$

Thus,

$$\frac{dG}{dN} = 0 = \frac{\cos \pi T_p N}{N^R} - R \frac{\sin \pi T_p N}{\pi T_p N^{R+1}}.$$

Solving for N,

$$\pi T_p N \cot \pi T_p N = R. \tag{36}$$

Consequently, it is the phase shift $\Phi = \pi T_p N$ which limits the coherent integration time. The solutions of Eq. (36) are

$$\Phi = 0.41, \quad \text{if} \quad R = 0.944, \tag{37a}$$

$$\Phi = 0.80, \quad \text{if} \quad R = 0.775, \tag{37b}$$

$$\Phi = 0.92, \quad \text{if} \quad R = 0.688, \tag{37c}$$

$$\Phi = 1.06, \quad \text{if} \quad R = 0.593, \tag{37d}$$

Thus, the limiting phase shift is seen to be a function of the number of noncoherent pulses that are integrated. To show that these results are valid in spite of the numerous approximations, the coherent gain equation, Eq. (29), and noncoherent gain equations, Eqs. (34), were programed on the CDC 3800 computer, and an exhaustive search was used to find the optimal value of N and Φ for the following parametric ranges:

$$f = 200 \text{ MHz},$$

$$\tau = 1.7122,$$

$$60 \leq \text{prf} \leq 240,$$

$$1 \leq T \leq 5.$$

The results of this investigation are shown in Table 14. One can infer from this data that when one is integrating a short time (a few noncoherent pulses) the limiting phase shift is about 0.8 radian; however, when the integration time is longer, the limiting phase shift is increased to 0.92 radian. These results are compatible with the results in Eqs. (37). The loss due to the phase shift, in comparison to no phase shift at all, is given by $\sin\Phi/\Phi$, which is 0.9 or -0.5 db if $\Phi = 0.8$ and is 0.87 or -0.6 db if $\Phi = 0.9$.

Table 14
Limiting Phase Shift Φ

prf	M = prf		M = 3 prf		M = 5 prf	
	N	Φ (radians)	N	Φ (radians)	N	Φ (radians)
60	11	0.78	11	0.78	12	0.86
80	14	0.77	14	0.77	16	0.88
100	18	0.80	18	0.80	20	0.89
120	21	0.79	21	0.79	24	0.90
140	24	0.77	24	0.77	28	0.91
160	28	0.80	28	0.80	32	0.91
180	31	0.79	31	0.79	36	0.92
200	35	0.80	35	0.80	40	0.92
220	38	0.79	38	0.79	44	0.92
240	41	0.79	41	0.79	48	0.92

DATA PROCESSING (S)

Optimal Integration Angle (U)

When a radar scans past a point target, the amplitudes of the returned pulse train are proportional to the square of the one-way antenna voltage gain pattern. Usually, one considers integration over the beamwidth θ_b (which is determined by the 3-db power points) and suffers a 1.6-db "scanning loss," which is based on an optimal integration

angle of 0.84 θ_{3} for a gaussian-shaped beam. However, these figures are based on the work of Blake (11), who assumed a noncoherent gain that obeys the half-power law. To extend the work to other laws, a slightly different approach than Blake's will be used.

Two beam shape patterns will be considered: a gaussian beam shape and a $\sin x/x$ beam shape; that is,

$$G_1(\theta) = e^{-1.38(\theta/\theta_3)^2}$$

and

$$G_2(\theta) = \frac{\sin 1.3916(\theta/\theta_3)}{1.3916(\theta/\theta_3)},$$

where θ is the angle measured with respect to the beam center, θ_3 is the angle of the half-power point, and the gain is normalized to unity at midbeam.

To find the optimal integration angle, one must formalize the detection problem as a test of a binary hypothesis. Therefore, consider the problem of testing for a known signal in white gaussian noise:

$$H_0: Z_i = \ldots, \quad i = 1, 2, \ldots, N$$

$$H_1: Z_i = \ldots,$$

where $N+1$ is the number of pulses integrated.

The null hypothesis, H_0, is the statement that only noise is present; and the alternative, H_1, is the statement that signal plus noise is present. The noise samples $\ldots$ and $\ldots$ are independent identically distributed gaussian random variables with mean zero and variance $\ldots$. Since we are mostly concerned with the threshold case (small S/N ratio), the square-law detector will be considered. That is, the test statistic

$$S_1 = \sum_{i=1}^{N} Z_i^2$$

will be compared to a threshold T. If $S_1 \geq T$, then H_1 is accepted (signal is present); and if $S_1 < T$, then H_0 is accepted. Since S_1 is equal to the sum of independent random variables, S_1 is essentially gaussian as implied by the central limit theorem. Thus, only the means and variances of S_1 under both hypotheses will be important in the detection problem. Consequently, it is necessary to calculate them. In the forthcoming calculations the following well-known information about the moments of a zero mean gaussian variable will be used:

$$E\{\ldots\} = \ldots$$

$$E\{\ldots\} = \ldots$$

$$E(x_i^3) = E(y_i^3) = 0 ,$$

$$E(x_i^4) = E(y_i^4) = 3\sigma^4 .$$

Then, the means of Z_i^2 are

$$E(Z_i^2 | H_0) = E\{x_i^2 + y_i^2\} = 2\sigma^2$$

and

$$E(Z_i^2 | H_1) = E\left\{[x_i + G^2(\omega_i)]^2 + y_i^2\right\} = G^4(\omega_i) + 2\sigma^2 ,$$

and the second moments are

$$E(Z_i^4 | H_0) = E(x_i^2 + y_i^2)^2 = 8\sigma^4$$

and

$$E(Z_i^4 | H_1) = E\left\{[x_i + G^2(\omega_i)]^2 + y_i^2\right\}^2 = G^8(\omega_i) + 8G^4(\omega_i)\sigma^2 + 8\sigma^4 .$$

The variances of Z_i^2 are

$$\mathrm{var}(Z_i^2 | H_0) = E(Z_i^4 | H_0) - [E(Z_i^2 | H_0)]^2 = 4\sigma^4$$

and

$$\mathrm{var}(Z_i^2 | H_1) = E(Z_i^4 | H_1) - [E(Z_i^2 | H_1)]^2 = 4\sigma^2 G^4(\omega_i) + 4\sigma^4 .$$

Since the mean of the sum of random variables is equal to the sum of the means of the random variables, and since the variance of the sum of independent random variables is equal to the sum of the variances of these random variables, one obtains

$$E(S_N | H_0) = \sum_{i=-N}^{N} 2\sigma^2 = 2\sigma^2(2N+1) , \tag{38}$$

$$E(S_N | H_1) = \sum_{i=-N}^{N} [G^4(\omega_i) + 2\sigma^2] = \sum_{i=-N}^{N} G^4(\omega_i) + 2\sigma^2(2N+1) , \tag{39}$$

$$\mathrm{var}(S_N | H_0) = \sum_{i=-N}^{N} 4\sigma^4 = 4\sigma^4(2N+1) , \tag{40}$$

and

$$\mathrm{var}(S_N | H_1) = \sum_{i=-N}^{N} [4\sigma^2 G^4(\omega_i) + 4\sigma^4]$$

$$= 4\sigma^2 \sum_{i=-N}^{N} G^4(\omega_i) + 4\sigma^4(2N+1) . \tag{41}$$

From these preliminaries, one can proceed to the heart of the problem. When making a test between two gaussian distributions, $G(\mu_1, \sigma_1^2)$ and $G(\mu_2, \sigma_2^2)$, the probability of detection is a monotonic function of the expression (as proved in Appendix A)

$$I = \frac{\mu_2 - \mu_1 - \sigma_1 \Phi^{-1}(1 - P_{fa})}{\sigma_2} , \tag{42}$$

where $\Phi(\cdot)$ is the cumulative distribution for a normalized gaussian (i.e., $G(0,1)$),

$$\Phi(x) = \int_{-\infty}^{x} \frac{1}{\sqrt{2\pi}} e^{-x^2/2} dx ,$$

and consequently $\Phi^{-1}(1 - P_{fa})$ is the threshold corresponding to a probability of false alarm of P_{fa}. Using the appropriate equivalences

$$\mu_1 = E(S_N | H_0) ,$$

$$\mu_2 = E(S_N | H_1) ,$$

$$\sigma_1 = [\mathrm{var}(S_N | H_0)]^{1/2} ,$$

and

$$\sigma_2 = [\mathrm{var}(S_N | H_1)]^{1/2} ,$$

substituting Eqs. (38) through (41) into Eq. (42) yields

$$I(N = K_0 K_2, G) = \frac{\sum_{i=-N}^{N} G^2(i = K) - 2^{-G} \sqrt{2N+1}\, \Phi^{-1}(1 - P_{fa})}{2^{-G} \left[\sum_{i=-N}^{N} G^2(i = K) + (2N+1)^{-G} \right]^{1/2}} , \tag{43}$$

where one receives K pulses per radian. That is,

$$N = K\theta_2 .$$

For a side-looking radar K can be expressed as

$$K = \frac{R \cdot \mathrm{prf}}{V} ,$$

where R is the target range and V is the velocity of the radar platform.

The optimal integration angle θ_2 is the angle that maximizes Eq. (43). It is quite obvious that the optimal θ_2 is a function of G and hence of the S/N ratio. However, it is surprising to note that the optimal θ_2 is also a function of the prf through the variable K.

Equation (43) was programed on the CDC 3800 computer with $\Phi^{-1}(1 - P_{fa}) = 6.232$,* ε varying from 0.4 to 0.9, and K varying from 0.005 to 0.05. The results for a $(\sin x)/x$ beam shape are shown in Table 15.

Table 15
Optimal Integration Angle θ_2 for a $(\sin x)/x$ Beam in θ_1 Units

$1/K$	θ_2 (radians) for Various S/N Ratios					
	4.95*	3.01	1.43	0.09	-1.07	-2.10
0.005	1.145	1.065	1.005	0.955	0.915	0.88
0.010	1.11	1.03	0.96	0.910	0.87	0.84
0.015	1.08	1.005	0.93	0.885	0.84	0.81
0.020	1.06	0.98	0.92	0.86	0.82	0.78
0.025	1.05	0.95	0.90	0.825	0.80	0.75
0.030	1.02	0.93	0.87	0.81	0.78	0.75
0.035	1.015	0.915	0.84	0.805	0.77	0.735
0.040	1.00	0.915	0.84	0.80	0.76	0.72
0.045	0.99	0.91	0.81	0.765	0.72	0.72
0.050	1.00	0.90	0.80	0.75	0.70	0.70

*$S/N = 10 \log(1.2^2)$.

The question naturally arises: If one integrates over the optimal angles given in Table 15 what is the scanning loss associated with the fact that the returning signals have a lower strength off midbeam? To calculate this scanning loss it is necessary to calculate the value of Eq. (43) for a rectangular beamwidth. Thus, if one lets $G = 1$, Eq. (43) becomes

$$I(N, K, \varepsilon, 1) = \frac{(2N \cdot 10^{[\quad]/10} - 2)^{\frac{1}{2}} \Phi^{-1}(1 - P_{fa})}{2 \cdot 1 \cdot \varepsilon^{N-1}} \quad (44)$$

The scanning loss for a particular N and P_{fa} will be defined as the change in the S/N ratio (i.e., the change in ε) required to equate Eq. (43) to Eq. (44).

To illustrate how the scanning loss is calculated, let us consider the case where $N = 61$. Equations (34) give an integration gain of 14.47 db for an integration of 61 pulses. Consequently, an S/N ratio of 1.53 db is required to obtain a 16-db integrated S/N ratio. Then, Eq. (43) was evaluated for ε values ranging from 0.8 to 1.0 and S/N ratios ranging from 2.73 to 3.53. The results are presented in Table 16.

*This threshold corresponds to $P_{fa} = 10^{[\quad]}$.

Table 16
Evaluation of Eq. (43) for $N = 61$

θ	Value of $I(N, K, \sigma, G)$								
	2.73*	2.83	2.93	3.03	3.13	3.23	3.33	3.43	3.53
0.80	0.298	0.310	0.323	0.336	0.349	0.362	0.375	0.388	0.401
0.82	0.290	0.302	0.315	0.328	0.340	0.353	0.366	0.379	0.392
0.84	0.282	0.294	0.307	0.319	0.332	0.345	0.358	0.371	0.384
0.86	0.274	0.286	0.299	0.311	0.324	0.336	0.349	0.362	0.375
0.88	0.266	0.278	0.291	0.303	0.316	0.328	0.341	0.353	0.366
0.90	0.259	0.271	0.283	0.295	0.307	0.320	0.332	0.345	0.357
0.92	0.251	0.262	0.275	0.287	0.299	0.311	0.224	0.336	0.349
0.94	0.243	0.255	0.267	0.279	0.291	0.303	0.315	0.328	0.340
0.96	0.235	0.247	0.259	0.271	0.283	0.295	0.307	0.319	0.331
0.98	0.227	0.239	0.251	0.263	0.275	0.286	0.298	0.211	0.323
1.00	0.220	0.231	0.243	0.255	0.266	0.278	0.290	0.302	0.314

*S/N = 10 log (1.2^5).

Since the value of Eq. (44) is 0.318 for $N = 61$, the required S/N ratios (which can be obtained by using linear interpolation on Table 16) are shown in Table 17.

Table 17
Required S/N Ratio for Eq. (43) to Equal 0.318 for $N = 61$

θ (radians)	S/N Ratio	Scanning Loss (db)	$1/K$
0.80	2.89	1.36	0.027
0.82	2.95	1.42	0.027
0.84	3.02	1.49	0.028
0.86	3.08	1.55	0.029
0.88	3.15	1.62	0.030
0.90	3.21	1.68	0.031
0.92	3.28	1.75	0.031
0.94	3.35	1.82	0.031
0.96	3.42	1.89	0.032
0.98	3.48	1.95	0.033
1.00	3.55	2.02	0.033

Since one should be integrating for the optimal time, the θ one should choose should correspond to an optimal θ for the particular $1/K$ used. Referring to Table 15, such a matching pair is $1/K = 0.031$ and $\theta = 0.92$. Consequently, the scanning loss for 61 pulses is about 1.75 db. This procedure was repeated for various N, and the results are shown in Table 18. Hence, both the optimal integration angle and scanning loss are a function of the number of pulses integrated.

Table 18
Scanning Loss and Optimal Integration Angle for Various N

Number of Pulses Integrated N	Scanning Loss (db)	Optimal Integration Angle θ_2 (radians)	Number of Pulses Integrated N	Scanning Loss (db)	Optimal Integration Angle θ_2 (radians)
61	1.75	0.92	201	1.55	0.91
101	1.63	0.92	401	1.42	0.88

Optimal Weighting (U)

In the previous subsection, the optimal integration angle for a uniform weighting was found for the case of a radar scanning past a point target; i.e., the amplitudes of the returning pulse train are proportional to the square of the one-way antenna voltage gain pattern. In this section, the optimal weighting function is numerically calculated.

To find the optimal weighting, let us consider the following binary hypothesis:

H_0: the Z_i consist of noise along, $S = 0$,

H_1: the Z_i consist of signal plus noise, $S \neq 0$,

where $\{Z_i\}$ are samples from the output of an envelope detector and S is the amplitude of a sinusoidal signal. Rice (12) calculated the probability densities to be

$$p(Z_i \mid S = 0) = \frac{Z_i}{\sigma_n^2} e^{-Z_i^2/2\sigma_n^2}$$

and

$$p(Z_i \mid S \neq 0) = \frac{Z_i}{\sigma_n^2} e^{-(Z_i^2+S^2)/2\sigma_n^2} I_0(Z_i S/\sigma_n^2),$$

The Neyman-Pearson Lemma states that the optimal decision rule should be based on the likelihood ratio $L_N(Z_i)$ given by

$$L_N(Z_i) = \prod_{i=1}^{N} \left[\frac{Z_i e^{-(Z_i^2+S^2)/2\sigma_n^2} I_0(Z_i S/\sigma_n^2)}{Z_i e^{-Z_i^2/2\sigma_n^2}} \right],$$

which reduces to

$$L_M(Z_i) = \prod_{i=1}^{M} e^{-S_i^2/2\sigma_0^2} I_0(Z_i S_i/\sigma_0^2) .$$

Since the exponential term is a constant, the likelihood ratio is a monotonic function of the product of the Bessel functions:

$$L_M(Z_i) = \prod_{i=1}^{M} I_0(Z_i S_i/\sigma_0^2) , \tag{45}$$

and this product is the optimal detector. However, this optimal detector is never implemented because of its cumbersome form. Rather, the usual approach is to expand the Bessel function in an infinite series:

$$I_0(x) = 1 + \frac{x^2}{4} + \frac{x^4}{64} + \cdots . \tag{46}$$

Substituting Eq. (46) into Eq. (45) yields

$$L_M(Z_i) = \prod_{i=1}^{M} \left(1 + \frac{Z_i^2 S_i^2}{4\sigma_0^4} + \frac{Z_i^4 S_i^4}{64\sigma_0^8} + \cdots \right) ,$$

which can be rewritten as

$$L_M(Z_i) = 1 + \frac{1}{4\sigma_0^4} \sum_{i=1}^{M} Z_i^2 S_i^2 + \frac{1}{128\sigma_0^8} \sum_{i=1}^{M} \sum_{j \neq i}^{M} (Z_i^2 S_i^2)(Z_j^2 S_j^2) + \cdots . \tag{47}$$

The usual small-signal argument is now employed; that is, if $(Z_i S_i/\sigma_0^2)^2$ is of the order of ε, the higher order terms of Eq. (47) can be neglected and only the single summation need be considered:

$$L_M(Z_i) = \sum_{i=1}^{M} Z_i^2 S_i^2 . \tag{48}$$

Equation (48) represents a fourth-power voltage-antenna-pattern weighting, since S_i is the square of voltage antenna pattern. This is in contrast to the usual weighting that is used — the squared weighting. Fortunately, much of the difficulty can be removed if one realizes that Eq. (48) is not a very good approximation to Eq. (47) unless the signals are *extremely* small. This is because even though the fourth-power terms are of the order ε^2, there are M^2 of these terms in comparison to the M terms of order ε. Thus, the optimal weighting (w_i) for a square law,

$$\sum_{i=1}^{M} w_i Z_i^2 , \tag{49}$$

is not S_i^2, since the fourth power terms which cannot be neglected depend on the squared terms. Consequently, it will be necessary to calculate (w_i).

The method of calculation is as follows: First, if expression (49) is used as our test statistic and if the calculations in the previous section are repeated, the probability of detection can be shown to be a monotonic increasing function of the quantity

$$l = \frac{\sum_{i=-N}^{N} w_i G^4(i\ k) - 2^{-2}\Phi^{-1}(1-P_{fa}) \left(\sum_{i=-N}^{N} w_i^2 \right)^{1/2}}{2^{-2} \left[\sum_{i=-N}^{N} w_i^2 G^4(i\ k) + 2^{-2} \sum_{i=-N}^{N} w_i^2 \right]^{1/2}} \qquad (50)$$

The optimal weighting pattern consists of the set of $\{w_i\}$ which maximizes Eq. (50). The optimal weighting was found by numerical methods, and the results are shown in Fig. 13. As one can readily see, the optimal weighting is neither the square-law or fourth-law but rather something in between. Also, the weighting is a function of the S/N ratio per pulse.

The question naturally arises as to how much improvement one obtains by using the optimal weighting instead of a $[(\sin x)/x]^2$ weighting or a uniform weighting. As summarized in Table 19 the results indicate that if one integrates over an interval ± 2, the optimal weighting is only 0.1 db better than the uniform weighting. Also, if one doubles the

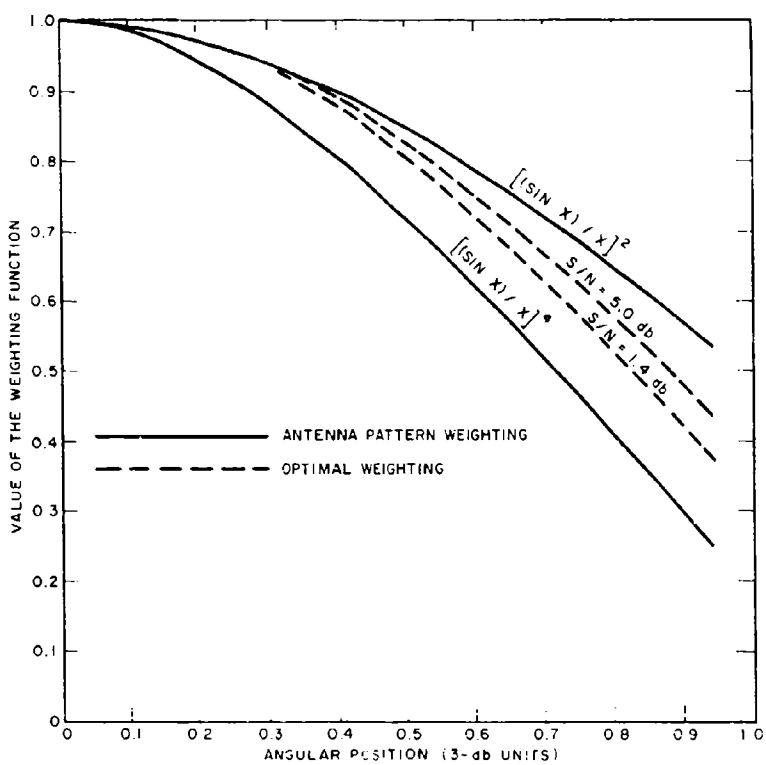

Fig. 13 - Weighting functions

integration interval (doubles the storage requirements), the optimal weighting is only 0.3 db better than the uniform weighting. Thus, the uniform weighting over the angle θ_2 is very close to the optimal condition.

Table 19
Output S/N Ratio for Different Weighting Patterns

Weighting Pattern	S/N (db) for Two Lengths of Integration Interval*	
	θ_2	$2\theta_2$
Uniform	15.7	14.6
$(\sin x)/x$	15.77	15.9
Optimal	15.8	16.0

*The input S/N ratio was 1.4 db per pulse, and θ_2 is the optimal integration angle for a uniform weighting.

Azimuthal Position Estimates (S)

The question considered in this subsection is the following: After a target has been detected, how close can its position be estimated in azimuth? The two estimators of position which are considered are shown in Fig. 14. The first estimator is

$$\hat{x} = \text{JMAX},$$

where JMAX is that j such that

$$S_N(\text{JMAX}) \geq \max S_N(j),$$

and the second estimator is

$$\hat{y} = (\text{JLAST} + \text{JFIRST})/2,$$

where JFIRST is the smallest j such that $S_N(j) \geq T$ and JLAST is the largest j such that $S_N(j) \geq T$.

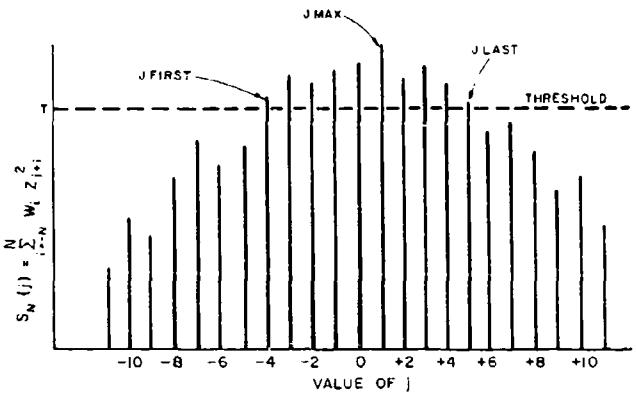

Fig. 14 - Azimuthal position estimates: JMAX and (JLAST + JFIRST)/2

While it is quite difficult to calculate the distributions of $\hat{x}$ and $\hat{y}$, a Monte Carlo study consisting of 1000 cases shows that $\hat{x}$ and $\hat{y}$ are both gaussian unbiased estimators. This inference can be arrived at from Figs. 15 and 16, in which a straight line indicates a gaussian distribution. Hence the variances of the estimators indicate the relative

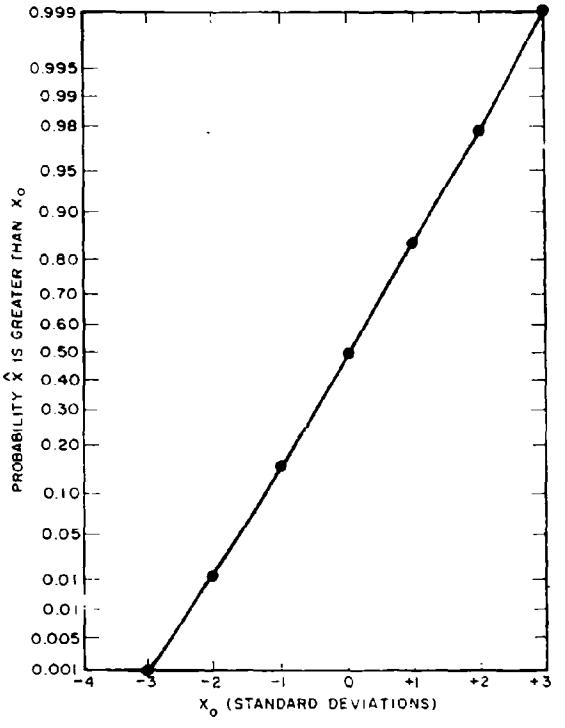

Fig. 15 - Distribution of $\hat{\gamma}$ [illegible]

goodness of the estimators. The standard deviations for a 1000-case Monte Carlo study are shown in Table 20. All the estimators are quite compatible in performance except for $\hat{\gamma}$ with a uniform weighting. One can make the following statement about azimuthal position: The interval

$$\hat{\gamma} - 2[\mathrm{Var}\,\hat{\gamma}]^{1/2} \text{ to } \hat{\gamma} + 2[\mathrm{Var}\,\hat{\gamma}]^{1/2}$$

or the interval

$$\hat{\psi} - 2[\mathrm{Var}\,\hat{\psi}]^{1/2} \text{ to } \hat{\psi} + 2[\mathrm{Var}\,\hat{\psi}]^{1/2}$$

Table 20
Standard Deviations of the Estimators $\hat{\gamma}$ and $\hat{\psi}$
for a 1000-Case Monte Carlo Study

Estimator	Standard Deviation for Different Weighting Patterns*		
	Uniform	[illegible]	Optimal
$\hat{\gamma}$	0.20	0.15	0.15
$\hat{\psi}$	0.15	0.13	0.13

* [illegible] is the angle to the half-power point.

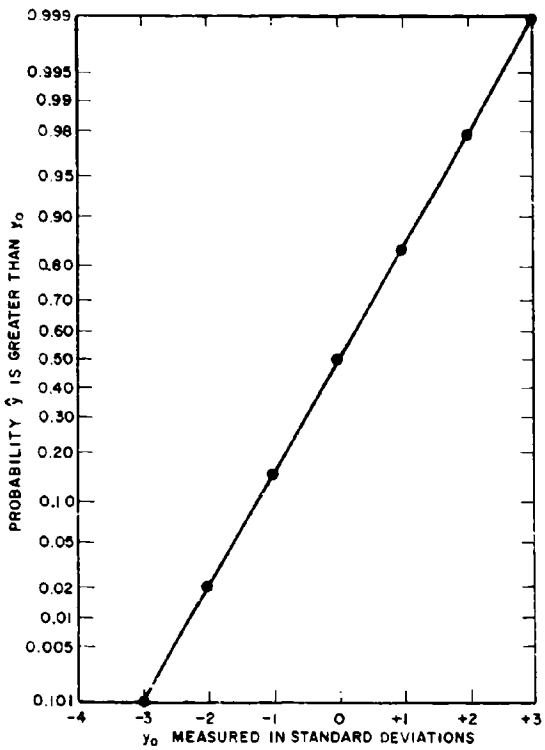

Fig. 16 - Distribution of $\hat{y} = (\text{JLAST} + \text{JFIRST})/2$

covers the true target azimuthal position 95 percent of the time. This means that with a beamwidth of 0.4 degree ($2\theta_{\frac{1}{2}}$ = 0.4 degree) and at a range of 2000 naut mi, 95 percent of the time the target can be located within the accuracies given in Table 21. The general formula for accuracy is

$$2R\sigma(\theta_{\frac{1}{2}})$$

where R is the range in nautical miles and $\sigma(\theta_{\frac{1}{2}})$ is the standard deviation of the estimator (given in Table 20) in terms of $\theta_{\frac{1}{2}}$ in radians, with $2\theta_{\frac{1}{2}}$ being the beamwidth.

Table 21
Azimuthal Position Accuracy With Which a Target
Can be Located 95 Percent of the Time

Estimators	Azimuthal Position Accuracy (naut mi) for Different Weighting Patterns		
	Uniform	$[\sin(\pi\theta/\theta_{\frac{1}{2}})/(\pi\theta/\theta_{\frac{1}{2}})]^2$	Optimal
$\hat{x}$	2.79	2.09	2.09
$\hat{y}$	2.09	1.81	1.81

All of the previous statements on azimuthal accuracy have been based on the assumption of an integrated S/N ratio of about 16 db. Obviously, larger targets will have a much larger integrated S/N ratio, and then better azimuthal accuracies result. For instance, for an output S/N ratio of 26 db with a uniform weighting the standard deviations of $\hat{x}$ and $\hat{y}$ are

$$[\mathrm{var}(\hat{x})]^{1/2} = 0.073\theta_1 \tag{51a}$$

and

$$[\mathrm{var}(\hat{y})]^{1/2} = 0.049\theta_1 \tag{51b}$$

Using Eqs. (51), the resulting azimuthal accuracies are 1.02 naut mi for $\hat{x}$ and 0.68 naut mi for $\hat{y}$ for an 0.4-degree beamwidth and a 2000-naut mi range.

The question arises: What is the maximum accuracy obtainable for the previous set of conditions? Fortunately, this question can be answered by making use of some previous work of Swerling (13). He showed (by using the Cramer Rea inequality) that the standard deviations of the optimal estimator were $\sigma_{\mathrm{opt}} = 0.11\theta_1$ for the 16-db case and $\sigma_{\mathrm{opt}} = 0.031$ for the 26-db case. These accuracies correspond to position errors of 1.53 naut mi for 16 db and 0.43 naut mi for 26 db. Thus, the two simple estimators are not too far off from the optimal estimator.

METHOD OF MAINTAINING A CONSTANT FALSE ALARM RATE (U)

Consideration of Different Methods (U)

It is usually assumed that the noise has a Rayleigh distribution. Unfortunately, in the surveillance problem, the radar will be limited by sea clutter at the large grazing angles as opposed to receiver noise (Rayleigh) limited at the shallow grazing angles. While one usually assumes a Rayleigh distribution for the sea clutter, it appears very unlikely that the noise has a Rayleigh distribution out to 6σ. (This corresponds roughly to a threshold for a $P_{fa} = 10^{-10}$.) Consequently, to maintain a $P_{fa} = 10^{-10}$ when one is clutter limited, one usually either uses adaptive schemes or else hard limits the data. Usually adaptive methods are used when the form of the noise distribution is known but certain of its parameters are unknown. For instance, if the noise is gaussian with a nonstationary unknown variance (noise power), the adaptive procedure is nothing more than a variable threshold which is proportional to the estimated noise power. Since the distribution of sea clutter is not only non-Rayleigh but also unknown, before conventional adaptive methods could be used, one would have to estimate the functional form of the density of sea clutter. Estimating this density out to 6σ or 7σ seems impossible. Hence, adaptive methods of this nature do not seem very promising.

On the other hand, hard limiting seems quite practical if one is integrating for a long time, i.e., accumulating 25 or more pulses. While hard limiting yields a constant false alarm rate, it results in a loss of about 2 db. (Further discussion of the hard limiting loss is given in Ref. 14.) Unfortunately, for certain types of processing, hard limiting also causes strong targets to interfere with the detection of weaker targets (15).

Thus, both adaptive and hard limiting methods have undesirable features. However, a method combining soft limiting and an adaptive threshold seems quite promising. This method is based on the fact that even though the density of sea clutter is nongaussian in the 6σ or 7σ region, it is almost gaussian below 2.5σ or 3σ. Hence, if one limits the data at 3σ (for instance), one now knows the density of sea clutter except for the noise power

. Thus, one can estimate and use this estimated value to control the value of the soft limiter and the decision threshold. An alternate way of accomplishing the same thing is to have a fixed value for the soft limiter and to have a fixed threshold. The estimated is used to control an agc so that the noise is always limited at its 3 point. An added advantage of a soft limiter is that it reduces the dynamic range required by the data processor.

Soft Limiting Loss (U)

While the hard limiting loss is fairly easy to calculate, the soft limiting loss is much more difficult to calculate. Marcum (16) defines the soft limiting ratio as the ratio of the limit level to the rms noise level. He concludes that if the number of pulses integrated is large, the limiting loss is only a fraction of a db if the limiting ratio is as large as 2 or 3, but that if only one or two pulses are integrated, the limiting ratio must be in the neighborhood of 10 to prevent a serious loss. Thus, while Marcum makes the qualitative statement that in certain cases the loss is small, he makes no quantitative statement about the loss, the limiting value, or the number of pulses integrated. Consequently, it was decided to investigate this problem further.

In attacking this problem, one could use the standard approach that employs the Gram-Charlier series; however, Marcum said the calculations were quite tedious. Alternately, one could calculate the probability distribution of the limited noise by the characteristic function method. Unfortunately, this results in a triple integral for which there exists no known closed form solution. A numerical integration of this triple integral to the desired accuracy would require an exorbitant amount of time on a digital computer; consequently, this method seems impractical also. Therefore, it was decided to use a Monte Carlo method to calculate the loss rather than use either of the two previous methods.

The system to be investigated by the Monte Carlo procedure is shown in Fig. 17. It consists of a soft limiter, followed by a dechirping device, followed by an envelope detector, followed by a -pulse accumulator whose output is compared to a threshold . The Monte Carlo procedure just consists in performing the operations shown in Fig. 18 which is the mathematical model of the system shown in Fig. 17. The main part of the simulation is the generation of the signal plus noise components and . The gaussian noise is generated by the equation

where is Rayleigh distributed and is uniformly distributed on (0, 2). Since a uniform random number generator is available on the computer which generates a random number uniformly distributed on (0, 1), generation of simply involves the multiplication of by 2 . The generation of is accomplished by the uniform random number generator in the following way:

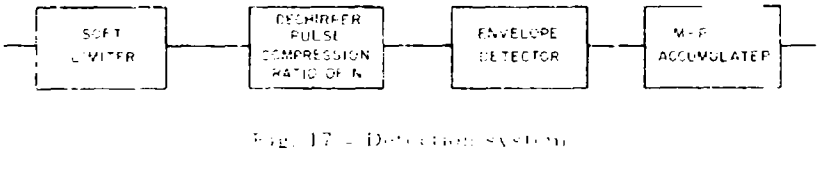

Fig. 17 – Detection system

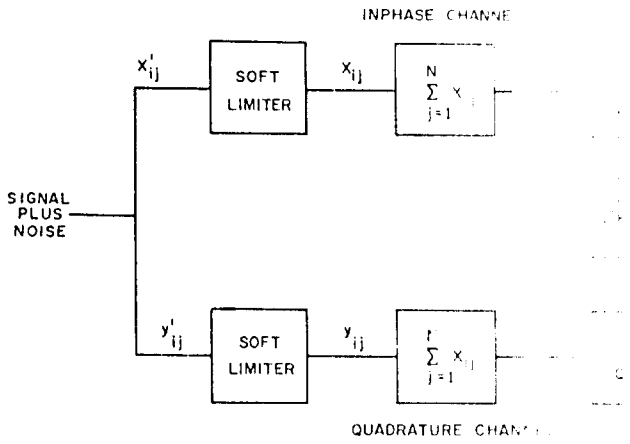

Fig. 18 - Mathematical model of the [illegible]

$$P(r \geq u) = \int_{u}^{\infty} r e^{-r^2/2} \, dr$$

Integrating, one obtains

$$P(r \geq u) = 1 - e^{-u^2/2}$$

or

$$e^{-u^2/2} = 1 - P \tag{52}$$

The quantity $1 - P(r \geq u)$ is uniformly distributed between 0 and 1 and consequently can be replaced by a random number r. Hence, if one solves Eq. (52) for u, one obtains

$$u = (-2 \ln r)^{1/2}$$

which shows that u has a Rayleigh distribution. Thus, one can generate the components x'_{ij} and y'_{ij} by generating two random numbers r_{ij} and r_{ij+1}; i.e.,

$$x'_{ij} = S + u_{ij} \sin \theta_{ij}$$

and

$$y'_{ij} = u_{ij} \cos \theta_{ij}$$

where

$$\theta_{ij} = 2\pi r_{ij+1}$$

and

$$u_{ij} = (-2 \ln r_{ij})^{1/2}$$

To find the limited components x_{ij} and y_{ij}, one first calculates the envelope e_{ij}:

$$e_{ij} = (x_{ij}^2 + y_{ij}^2)^{1/2}.$$

If $e_{ij} \leq$ SL (soft limiting value), then $x_{ij} = x'_{ij}$ and $y_{ij} = y'_{ij}$. On the other hand, if $e_{ij} >$ SL, then $x_{ij} =$ SL$(x'_{ij})\ e_{ij}$ and $y_{ij} =$ SL$(y'_{ij})\ e_{ij}$.

After the soft limiter, the simulation process is straightforward. One generates N pairs of pulses in a similar manner, sums up these N pulses, squares the two sums, adds the two squares, and takes the square root — this represents the output of an envelope detector of a dechirped pulse. Finally, one sums M of the dechirped pulses and compares the sum to a threshold T.

Finally, the system was simulated on the CDC 3800 with the following input parameters: $N = 63$, $M = 128$, $S = 0.13515$, $\sigma = 1$, and $T = 1620$. The threshold was set to yield a probability of false alarm of 10^{-8} and a probability of detection of 0.5. The results of the Monte Carlo procedure are shown in Table 22.

Table 22
Results of the Monte Carlo Procedure Shown in Fig. 18

Limit Value	No. of Cases	No. of Correct Decisions	Probability of Detection	Estimated S/N Ratio	Loss (db)
∞	107	57	0.532	-2.3	–
3.0	107	49	0.458	-2.5	0.2
2.5	107	27	0.252	-3.0	0.7
2.0	59	2	0.018	-4.0	1.7

The 100 cases or so that were run provide a good estimate of the probability of correct decision. However, one billion cases would have to be run if one wanted to calculate the probability of false alarm. But, since the inequality $P_{fa} \leq 10^{-8}$ is true, one can bound the soft limiter loss by setting $P_{fa} = 10^{-8}$ for all limit values. The estimated S/N ratios are found by finding the S/N ratios that yield the P_d values in Table 22 when one integrates 128 pulses. The S/N ratios were found using Robertson's curves (17). Consequently, the losses for limiting values of 3 σ, 2.5 σ, and 2 σ are bounded by 0.2, 0.7, and 1.7 db respectively. Thus, as long as one is limiting above 2.5 σ, the loss is lower than 0.7 db; and it is this author's opinion that the actual loss is about 0.2 db.

REFERENCES

1. Middleton, D., "An Introduction to Statistical Communication Theory," New York: McGraw-Hill, 1960

2. Rubin, W.L., and Difranco, J.V., "Radar Detection," Electro-Technology 73(No. 4): 63-90 (Apr. 1964)

3. Vine and Volkmann, Woods Hole Oceanographic Institute, June 1950

4. Swerling, P., Rondinelli, L.A., and Brennan, L.E., Technology Service Corporation Technical Report TSC-PD-009-1 (Secret), Mar. 1968

5. Guarguaglini, P.F., "A Unified Analysis of Diversity Radar Systems," IEEE Trans. on Aerospace and Electronic Systems, AES-4:318-320 (Mar. 1968)

6. Ellis, R.E., "Ocean Surveillance Radar Parametric Analysis," NRL Memorandum Report 1862 (Secret Report, Unclassified Title), Apr. 1968

7. Macdonald, NRL Electronics Division Technical Memorandum 5270-20, Aug. 23, 1966

8. Macdonald, NRL Electronics Division Technical Memorandum 5270-22, Sept. 7, 1967 (Confidential)

9. Fox, C.E., NRL unpublished memorandum, July 1967

10. Skolnik, M.I., "Introduction to Radar Systems," p. 37, New York:McGraw-Hill, 1962

11. Blake, L.V., "The Effective Number of Pulses Per Beamwidth for a Scanning Radar," Proc. IRE 41:770-774 (June 1953)

12. Rice, S.O., "Mathematical Analysis of Random Noise," Bell System Tech. J. 23:282-332 (1944) and 24:46-156 (1945)

13. Swerling, P., "Maximum Angular Accuracy of a Pulsed Search Radar," Proc. IRE 44:1146-1155 (Sept. 1955)

14. Trunk, G.V., NRL Radar Division Technical Memorandum 5308-103, Sept. 14, 1967

15. George, S.F., Sledge, O.D., and Abel, J.E., NRL Report 6443, "Cross Modulation in the SCAMP Signal Processor," Nov. 21, 1966

16. Marcum, J.I., "A Statistical Theory of Target Detection by Pulsed Radar: Mathematical Appendix," IRE Transactions on Information Theory IT-6:145-267 (Apr. 1960)

17. Robertson, G.H., "Operating Characteristics for a Linear Detector of CW Signals in Narrow-Band Gaussian Noise," The Bell System Tech. J. 46:755-774 (Apr. 1967)

Appendix A (U)

DERIVATION OF EQ. (42)

Given two gaussian distributions, $G(\mu_1, \sigma_1^2)$ and $G(\mu_2, \sigma_2^2)$, representing the null hypothesis and the alternative, the probability of false alarm is

$$P_{fa} = \int_T^\infty G(\mu_1, \sigma_1^2)\, dx, \tag{A1}$$

and the probability of detection is

$$P_d = \int_T^\infty G(\mu_2, \sigma_2^2)\, dx, \tag{A2}$$

where T is the threshold. Equations (A1) and (A2) can be rewritten as

$$1 - P_{fa} = \int_{-\infty}^{(T-\mu_1)/\sigma_1} G(0,1)\, dx = \Phi[(T-\mu_1)/\sigma_1] \tag{A3}$$

and

$$P_d = \int_{(T-\mu_2)/\sigma_2}^\infty G(0,1)\, dx. \tag{A4}$$

One may imply from Eq. (A4) that P_d is a monotonic increasing function of the quantity $(\mu_2 - T)/\sigma_2$:

$$P_d = F[(\mu_2 - T)/\sigma_2], \quad F \uparrow. \tag{A5}$$

Solving Eq. (A3) for T, one obtains

$$T = \mu_1 + \sigma_1 \Phi^{-1}(1 - P_{fa}). \tag{A6}$$

Substituting Eq. (A6) into Eq. (A5) yields

$$P_d = F\left\{[\mu_2 - \mu_1 - \sigma_1 \Phi^{-1}(1 - P_{fa})]/\sigma_2\right\}, \tag{A7}$$

where F is a monotonic increasing function.

SECRET
Security Classification

DOCUMENT CONTROL DATA - R & D

(Security classification of title, body of abstract and indexing annotation must be entered when the overall report is classified)

1. ORIGINATING ACTIVITY (Corporate author)
Naval Research Laboratory
Washington, D.C. 20390

2a. REPORT SECURITY CLASSIFICATION
Secret

2b. GROUP
3

3. REPORT TITLE
OCEAN SURVEILLANCE STATISTICAL CONSIDERATIONS(U)

4. DESCRIPTIVE NOTES (Type of report and inclusive dates)
A final report on one phase of the problem.

5. AUTHOR(S) (First name, middle initial, last name)
Gerard V. Trunk

6. REPORT DATE	7a. TOTAL NO. OF PAGES	7b. NO. OF REFS
November 27, 1968	52	17

8a. CONTRACT OR GRANT NO	9a. ORIGINATOR'S REPORT NUMBER(S)
NRL Problem R02-46	NRL Report 6804
b. PROJECT NO A375-38-006/6521/F019-02-01	
c.	9b. OTHER REPORT NO(S) (Any other numbers that may be assigned this report)
d.	

10. DISTRIBUTION STATEMENT
In addition to security requirements which apply to this document and must be met, each transmittal outside the Department of Defense must have prior approval of the Director, Naval Research Laboratory, Washington, D.C. 20390.

11. SUPPLEMENTARY NOTES	12. SPONSORING MILITARY ACTIVITY
	Department of the Navy (Naval Air Systems Command), Washington, D.C. 20360

13. ABSTRACT [Secret]

Several statistical topics were studied concerning detection of targets on the ocean's surface from a satellite-based radar. First, a desired signal-to-noise ratio was obtained by considering the tradeoff between false alarms and detected targets. For a 0.99 detection probability and a 10^{-10} false alarm probability the S/N ratio would be 16 db for a nonfluctuating target. Second, the decorrelation times of sea clutter were calculated and found to be so small that for side-looking radars sea clutter samples are independent from pulse to pulse but found to be so large for forward-scanning radars that one finally obtains decorrelation from sea motion instead of from platform motion. Third, a fluctuating target was considered, and the losses were calculated and compared with those of a nonfluctuating target. Roughly, one needs 1 to 4 db more power to detect a fluctuating target as opposed to a nonfluctuating target. Then, the ionosphere was considered, and the effects of Faraday rotation and the random phase shift were calculated. Degradation varies from intolerable below 900 MHz to negligible at 3 GHz. Next, some of the aspects of data processing were studied; the optimal integration angle was found, the optimal weighting was calculated, and azimuthal position estimators were considered. Surprisingly, optimal weighting gives a pattern only 0.3 db better than uniform weighting. Finally, a way was determined of using an adaptive threshold and soft limiting to maintain a constant false alarm rate.

DD FORM 1 NOV 65 1473 (PAGE 1)
S/N 0101-807-6801

SECRET
Security Classification

14 KEY WORDS	LINK A		LINK B		LINK C	
	ROLE	WT	ROLE	WT	ROLE	WT
Ocean surveillance						
Mathematical analysis						
Statistics						
Decorrelation times						
Fluctuating targets						
Ionospheric effects						
Optimal integration angle						
Optimal weighting						
Azimuthal position estimates						
Soft limiting						